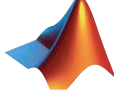
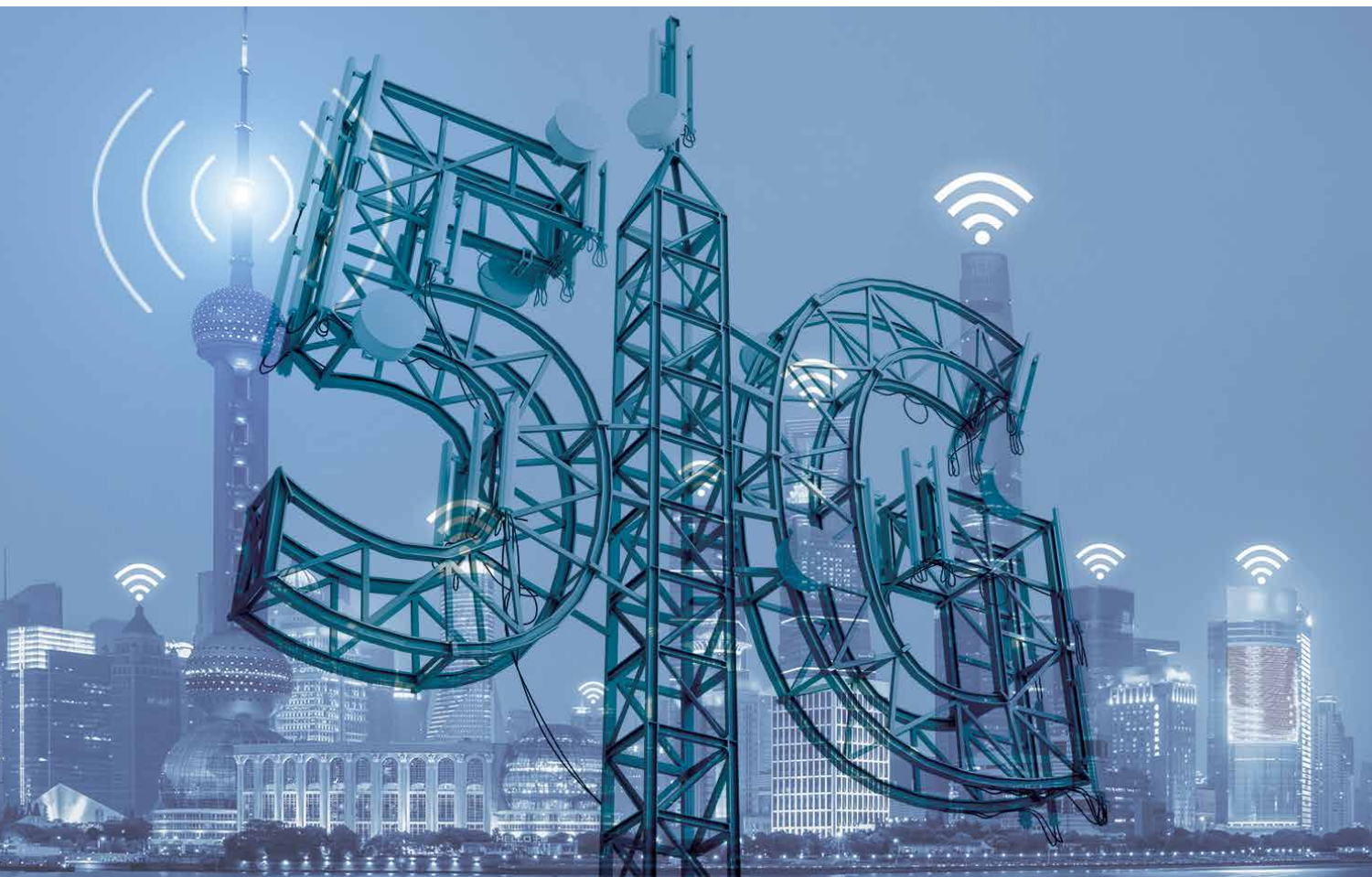


5G Phased Array Technologies

September 2019

SPONSORED BY  **MathWorks®**



3 Introduction

Pat Hindle
Microwave Journal, Editor

4 mmWave Will Be The Critical 5G Link

Joe Madden
Mobile Experts, Campbell, Calif.

8 All-Digital Antennas for mmWave Systems

Mike Kappes
IQ-Analog Corporation, San Diego, Calif.

12 Exploring Hybrid Beamforming Architectures for Massive MIMO 5G Systems

MathWorks

19 Adopting the 64 to 71 GHz Band for Fixed Wireless Applications

Sivers IMA
Kista, Sweden

23 Gapwaves Platform Integrates 5G mmWave Arrays

Carlo Bencivenni, Thomas Emanuelsson and Magnus Gustafsson
Gapwaves AB, Gothenburg, Sweden

30 Multi-Beam Phased Array with Full Digital Beamforming for SATCOM and 5G

Divaydeep Sikri and Rajanik Mark Jayasuriya
SatixFy UK Ltd., Farnborough, U.K.

5G Phased Array Technologies

Communication architectures are rapidly changing as commercial phased arrays are hitting the market for 5G and satellite applications. While these systems have been used for many years in the military, they were too expensive for commercial applications in the past. However, many companies have recently pioneered new architectures and semiconductor technologies to greatly reduce the cost and complexity of phased arrays making them available to commercial markets. Much of the impetus for this was the release of mmWave frequencies for 5G so many companies are rushing into the market for fixed wireless access and front/backhaul equipment for 5G.

This eBook takes a look at some of the innovative approaches to 5G phased arrays and the design/simulation to realize these products quickly. The eBook starts with an overview of the mmWave 5G market and technology approaches. Then efficient design and simulation techniques are covered to realize phased array designs. MathWorks then explores hybrid beamforming architectures for Massive MIMO 5G Systems including how use modeling and simulation to help reduce the risk associated with a complex workflow. Finally, several different architectures and approaches to 5G phased arrays are covered with solutions from IQ-Analog, SiverIMA, Gapwaves and StaixFy.

This eBook is aimed at providing an overview of some of the new approaches to realize 5G phased arrays and how to design/simulate them quickly to reduce time to market. We thank MathWorks for sponsoring this eBook to bring it to you at no cost.

Pat Hindle, Microwave Journal Editor



mmWave Will Be The Critical 5G Link

Joe Madden
 Mobile Experts, Campbell, Calif.

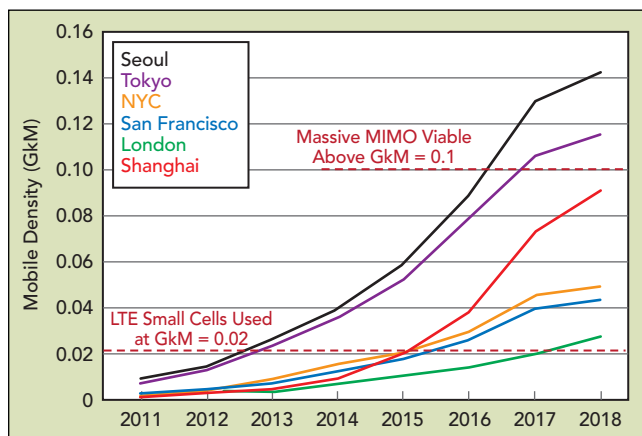
Over the past 30 years, the mobile network has become a critical part of life, and the use of mobile services is starting to reach incredible levels of demand. This year, 30 Exabytes will fly over worldwide mobile networks every month. And the demand will continue to rocket upward by roughly 50 percent each year. About 15 percent of adults in the U.S. use LTE full-time, leaving Wi-Fi turned off (they say that managing Wi-Fi hotspots can be annoying). A whole generation of young people consumes 50 GB of mobile video each month, relying on “unlimited plans.” The signs are clear that data demand will continue to grow rapidly.

Mobile Experts tracks the demand for mobile data with multiple mobile operators worldwide and their Traffic Density tracking metric measures the level of traffic in a busy sector, during busy hours, in terms of Gigabits per second, per square kilometer, per MHz of spectrum (GkM). In order to understand how advanced networks should handle extreme demand in some cities, the GkM is compared between different operators, and an assessment can be made whether small cells, massive MIMO or mmWaves will be necessary to accommodate the traffic (see **Figure 1**).

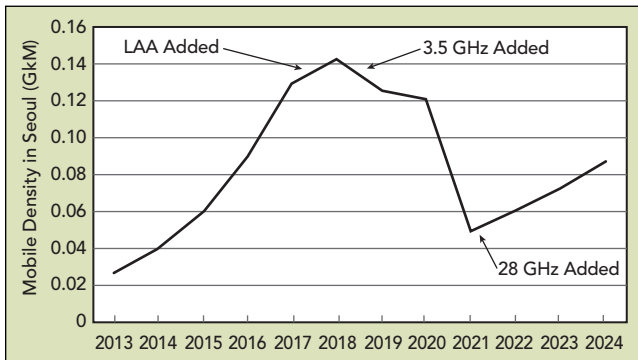
Traffic density in GkM has been rising steadily for years, and is most pronounced in locations such as subway stations in Tokyo and Seoul, where thousands of people stand close together, all watching video. The statistical rise in density has been remarkably smooth as new apps and video content become available on mobile platforms.

Above a traffic density level of 0.02 GkM, small cells were observed to be universally adopted by mobile operators. In other words, the macro network saturated above 0.02 GkM, and small cells became a more economical way to add capacity. More recently, networks have reached levels of density above 0.1 GkM, making massive MIMO necessary to continue increasing capacity.

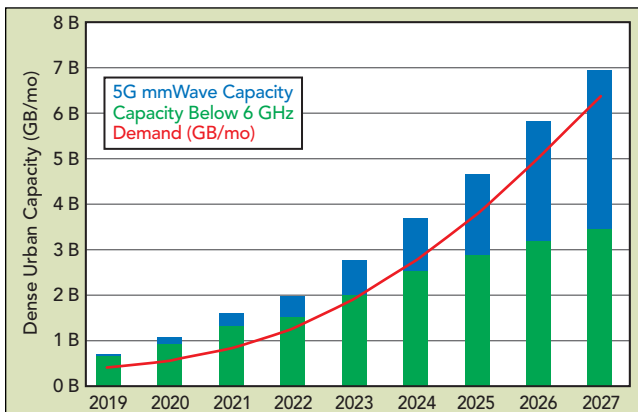
We are now starting to see some signs that density levels in the range of 0.15 to 0.2 GkM will saturate the OFDM network. There will be ways to push through this barrier as well, but moving beyond 0.2 GkM in the 1



▲ Fig. 1 Benchmarking data for Mobile Traffic Density (Gbps/km²/MHz or GkM).



▲ Fig. 2 Changes in traffic density with addition of 5G spectrum.



▲ Fig. 3 Demand vs. capacity for dense urban mobile networks in U.S.

to 3 GHz bands will get very expensive, requiring large numbers of very low-power radio nodes.

Adding 5G spectrum to the mobile network can actually reduce the traffic density. As an example, one of the leading Korean networks should experience a drop in GkM with their recent introduction of 100 MHz at 3.5 GHz. An additional 800 MHz of spectrum at 28 GHz will reduce their traffic density in key hotspots to much more manageable levels as shown in **Figure 2**.

Therefore in many ways the operators can be viewed as using 5G spectrum to manage the density of their traffic. When high density makes adding capacity expensive, adding more spectrum is the best option.

mmWAVES TO THE RESCUE

After the convenient licensed bands below 5 GHz are used up, mobile operators start to look to mmWave spectrum as an opportunity to get significant bandwidth. The U.S. is a prime example where wide blocks of C-Band spectrum are not available so mobile operators have invested heavily in 28 and 39 GHz mmWave bands.

In fact, the large U.S. mobile networks, in key urban pockets, are running out of capacity below 6 GHz. During special events such as the Super Bowl, the traffic density is in the range of 0.12 GkM and above in the U.S. Mobile Experts modeled the demand for mobile data in four segments of the U.S. network (dense urban, urban, suburban and rural) and estimated the total capacity of the mobile network including macro base stations, small cells, CBRS, LAA and the impact of massive

MIMO below 6 GHz. Even with a fully utilized heterogeneous network with maximal capacity, demand in dense urban pockets will exceed capacity in 2023 as shown in **Figure 3**. Note that the numbers shown in the Figure 3 represent the total demand and capacity for all dense urban sites in the U.S., so the extreme high-density locations such as Times Square will experience demand higher than capacity in the 2021 to 2022 timeframe. Extrapolating the trends in traffic density benchmarks, the dense urban sites in New York City should reach daily peak-hour density levels in the range of 0.1 GkM or higher by 2022.

HOW mmWAVE LINKS CAN BE USEFUL

Many experienced RF engineers have reasonable doubts about using mmWave radio links in a mobile environment. After all, the mmWave link depends on a narrow beam in order to achieve a reasonable link budget. Any clutter in the RF channel can disrupt the narrow beam.

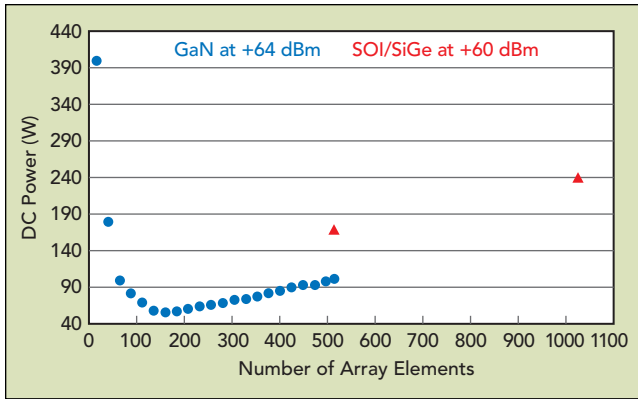
Handovers in a mobile 5G mmWave network have been demonstrated in test systems in Seoul and at speeds above 200 km/hr on a racetrack, so the 5G frame structure lends itself to handovers in extreme Doppler shift conditions.

However, the mobile operators will not be using the 5G mmWave link as a standalone (SA) radio channel initially. Instead, an LTE carrier at 1 to 2 GHz will be used as the primary link, with control signaling taking place on the more reliable lower band. Then, the mmWave link will come into play when it is available to download or upload large amounts of data. In this way, the mmWave radio will add throughput as a carrier aggregation layer, boosting speed when it is available but not essential to the continuity of the link for handovers. At some point, operators may decide to use 5G mmWave as a SA mobile network, but today none of the active operators are planning to operate 5G mmWave independently.

RF IMPLEMENTATION—INFRASTRUCTURE

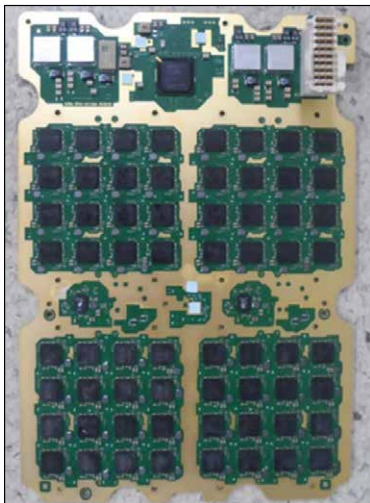
The mmWave base station will look dramatically different than LTE base stations below 6 GHz. At a fundamental level, the mmWave radio suffers from the lower power amplifier efficiency in the 24 to 40 GHz bands, so the level of conducted output power will be much lower than lower frequency mobile radios. The primary limitation is the level of heat dissipation possible in a passively cooled radio unit at the towpertop. Given a limit of about 250 W of heat in a small enclosure, the conducted RF power will be very low, below 10 W in any configuration.

As a result, systems engineers have turned to massive MIMO architectures with at least 64 antennas, in order to use high antenna gain. Initial products have utilized between 64 and 256 antenna elements per beam, to achieve between 25 and 30 dBi of antenna gain. In this way, the low conducted power can achieve linear EIRP in the range of 60 dBm. Each beam also carries multiple streams. Massive MIMO base stations are configured with dual-polarized antenna arrays, so that each beam can operate with 2x2 MIMO.



▲ Fig. 4 Comparison of power dissipation in GaN, SOI and SiGe arrays.

Multiple beams can be supported from a radio unit by constructing the array with multiple panels. From a manufacturing point of view, OEMs are settling into the use of panels with a set number of elements (examples range from 64 to 256 elements per panel). Then, the product can be scaled up and down to support different levels of capacity. One example in the field now uses four 256-element panels for a total of 1024 antenna elements, supporting four beams and 2x2 MIMO in each beam.

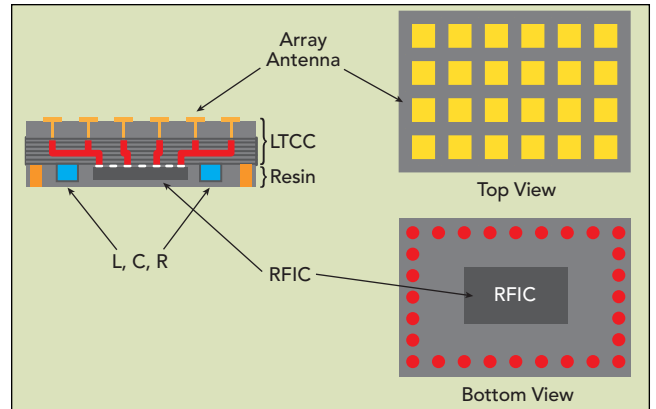


▲ Fig. 6 A typical panel with 4 sections, 64 256 dual-polarized antennas total (Source: FCC filing).

Note that the configuration of beams and streams is not set based on hardware. The OEM can choose to change the configuration in software, assuming that the antenna elements are equipped with analog phase shifter and variable gain components that can be individually controlled. In almost all prototypes, this “hybrid beamforming” approach is used today, as full digital beamforming at very wide bandwidths can be costly in terms of processing power and dollar cost.

Currently, SOI and SiGe semiconductor technologies are used in many base stations in order to achieve high levels of integration and low-cost. GaN also holds great potential for lower power dissipation at high levels of EIRP, using the higher inherent linearity/power of GaN devices to achieve 60 dBm or higher with fewer antenna elements.

Based on PA efficiency data and size/efficiency of heatsinks for live demonstrations at MWC Barcelona 2019, the DC power consumption of multiple mmWave arrays was estimated as shown in **Figure 4**. It appears that GaN has a significant advantage in terms of raw efficiency of a linear power amplifier at 28 GHz. However, all major OEMs have chosen to use SOI or SiGe so far,



▲ Fig. 5 A diagram representing physical packaging/integration for mmWave front ends (source: pSemi).

to take advantage of higher levels of integration, larger wafers and the resulting lower cost profile.

Over the next five years, significant adjustments are expected to occur to the balance between narrow beams (for long range) and wide beams (for better mobility). The optimal tradeoff in a dense urban network is not well understood today, and is likely to break into specific configurations to handle trains/buses/moving vehicles differently than pedestrian users. In particular, the large SOI-based arrays are expected to support the applications that cover dense urban pockets, where both vertical and horizontal steering are required and pedestrian speeds are typical. Other applications with higher mobility and less vertical steering are likely to move toward GaN devices.

The physical integration of the RF front-end will also be critical. Very tight integration will be necessary in the 24 to 40 GHz bands to keep insertion losses low, so either LTCC or 3D glass structures will be used to embed the active die and passive elements (see **Figure 5**).

In the Radio Unit (RU), one convenient arrangement is to use an RFIC device for four antenna elements. From a simple geometric point of view, one RFIC for beam-forming (phase and amplitude adjust) can be positioned between four antenna elements, using short traces and vias to route the mmWave signal (see **Figure 6**).

One open question concerns the use of filters in the mmWave front-end. Currently, no bandpass filters are used at the front-end, and during field trials the spectrum was clean enough to rely on the natural rolloff of the patch antenna and distributed antenna feed to provide out-of-band rejection. In the future, spectrum auctions and multi-operator deployment suggest that interference will arise. In fact, with high EIRP and very narrow beams, the interference will be intense when it unexpectedly pops up. Recent analysis indicates that filters will be introduced into the packaging over the next three years.

RF IMPLEMENTATION—CPEs

In fixed wireless, the Customer Premises Equipment (CPE) is a key part of the system. Initial deployments of 5G mmWave networks rely on high antenna gain and high EIRP from the CPE in order to support the necessary capacity. CPE RF front-ends today are constructed

using a method that is similar to the network infrastructure, with a panel of antenna elements supported by beamforming RFICs, up-/down-conversion and then baseband processing. A typical CPE uses 32 dual-polarized antenna elements, supporting 2x2 MIMO with about 20 dBi gain from the antenna system.

Because the CPE is always connected to prime power, the PA efficiency is not a crippling limitation, and the CPE can often achieve high gain and high transmit power (linear EIRP in the range of 40 dBm).

RF IMPLEMENTATION—HANDSETS AND OTHER MOBILE DEVICES

The biggest challenge facing the 5G mmWave link will come from the user's hand blocking the antennas on a smartphone. In the 28 GHz band, the user's hand is likely to attenuate the signal by at least 30 to 40 dB, effectively killing the link altogether. There can be multiple strategies to avoid this issue:

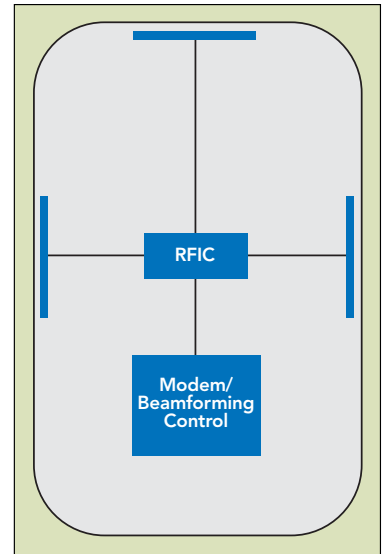
1. Multiple antenna sub-arrays on each handset. All 5G mmWave handset prototypes demonstrated over the past year utilize multiple sub-arrays, placed on both sides of the smartphone.
2. Foldable handsets are coming to market such as Samsung's Galaxy Fold and Huawei's Mate X. Because a foldable handset would be much larger than a human hand in the unfolded position, the placement of antennas could be more exposed.
3. Mobile hotspots can be used instead of mmWave links directly to the smartphone. This avoids the hand issue altogether, but may incur greater interference in the unlicensed bands. Importantly, the space and battery size constraints of the smartphone do not apply here, so the number of antennas can be increased to achieve much higher EIRP.

The physical implementation on a handset is limited for cost and space reasons to a few sub-arrays, an RFIC and the modem/beamforming processing. To make this arrangement economical, each mmWave sub-array includes an up-/down-converter to shift the mmWave signal down to an IF frequency at roughly 4 to 6 GHz (see **Figure 7**). This enables the signals to travel through the PCB to a centralized RF transceiver.

Each mmWave subarray currently uses four dual-polarized patch antennas, each with a transmit/receive switch, low noise amplifier (LNA) and power amplifier (PA) closely integrated using RF-SOI. Each amplifier can only produce about 15 dBm linear power, so as many as eight antennas would be used to reach EIRP levels somewhere above 20 dBm. Three-dimensional beamforming on the smartphone platform is challenging, especially with a cluttered environment with metal surfaces and human hands in very close proximity. Even with eight antennas engaged, prototyping so far suggests antenna gain of only about 5 dBi.

For that reason, we expect much higher performance with hotspot products that utilize 32 antennas or more, achieving gain in the range of 20 dBi in the antenna system (15 dBi from the array and 5 dBi from the patch antenna itself). This type of product should be

able to reach roughly 35 dBm linear EIRP or higher. From a system point of view, roughly 35 dBm or higher will be an important level to reach since the 5G link requires a closed loop with TDD channel feedback in order to maintain a continuous connection. Lower EIRP from the client device means a shorter range for the link, and would require the network operator to deploy larger numbers of cell sites in order to blanket a neighborhood with coverage. In short, low transmit power from the client devices would make the 5G business case unworkable for the mobile operator.



▲ Fig. 7 Layout of three mmWave sub-arrays on a handset.

COMMERCIAL STATUS

Base station deployment is underway in earnest for the U.S. market this year, and the South Korean market is not far behind. Recent forecasts indicate that more than 600,000 radio heads will be deployed by 2024.

Commercial fixed-wireless services have already been launched in a handful of U.S. cities, with CPEs supported by major OEMs today. A few CPEs have appeared from the ODM community with poor performance, but we expect those to improve quickly to support healthy growth. In the next few years, the fixed-wireless application will account for millions of users.

This generation of technology is also unique in that handsets are coming out very quickly, and smartphones will be available before the network is launched in most countries. The first 5G mmWave handset has already been released (the 5G Moto MOD), and at least eight other mmWave handsets will be released in the second half of 2019.

SUMMARY

5G mmWave radio links are more complex, more expensive and less reliable than LTE connections at 1 to 2 GHz. But mmWave bands will be necessary to keep up with rising demand, so the industry is currently pouring money into deployment of base stations and development of client devices. Initial fixed-wireless performance with CPEs has been surprisingly solid. The migration to mobile 5G usage will be tricky, with tradeoffs on beamwidth, link budget, mobility and cost coming into play. But there is one clear conclusion: 5G mmWave will be a significant part of future mobile networks. ■

All-Digital Antennas for mmWave Systems

Mike Kappes

IQ-Analog Corporation, San Diego, Calif.

To realize high performance mmWave communications, beamforming antenna systems will need to be smarter, faster, smaller, lower power, cost less, have lower latency and be easier to integrate than current technologies. Much like with previous telecommunication systems, integrating important processing and signal conditioning functions will enable more cost-effective and compact mmWave beamforming antennas. The development of complex mmWave RF and analog hardware for 5G and tactical communications will initiate an inevitable evolutionary trend in digital communications, with digital processing eventually supplanting analog. The recent emergence of an all-digital antenna approach leveraging antenna processing units (APU) and ASICs could accelerate this trend, further reducing the time-to-market for highly anticipated multi-data path mmWave 5G and tactical communications.

The limited bandwidth and abundant congestion of sub-6 GHz spectrum has spurred extensive investigation into additional swaths of spectrum from 20 GHz to over 100 GHz (i.e., mmWave) for next-generation wireless communication systems. Originally sought after by industrial and commercial organizations for 5G, interest in the mmWave spectrum has expanded to encompass military and aerospace applications, such as tactical communications.¹⁻³ Beyond a manifold increase in the available bandwidth, compared to the sub-6 GHz spectrum, mmWave frequencies present a variety of benefits, as well as a range of design and operational challenges.

The size of antennas and transmission lines at mmWave frequencies are smaller than those at sub-6 GHz, owing to the shorter physical wavelength, with the smaller size enabling much more compact hardware. Moreover, the beamwidths of mmWave antennas are much narrower, hence more spatially selective than lower frequency antennas. These benefits come with the trade-off of higher RF path loss and less efficient transmission. Additionally, the atmospheric attenuation at mmWave frequencies is much higher than in the sub-6 GHz bands. The reduced signal dispersion limits interference, jamming and potential snooping to roughly line-of-sight, offering benefits for tactical communications.

To overcome the greater RF path loss and atmospheric attenuation, it is widely accepted that the use of beamforming antenna technologies is one of the most

viable solutions.⁴⁻¹¹ Certain beamforming designs also enable active antenna features, such as active electronically scanned arrays (AESA), which have been instrumental in jamming, anti-jamming, SATCOM and aerospace communications systems.

Many research, industry and military organizations are investigating and developing mmWave active antenna technologies that can be deployed in a reliable and cost-effective manner. Cost, size and complexity are significant factors for mmWave communications systems, especially for 5G, as the range and coverage provided by small cells is intrinsically less than the prior generation macro cells, meaning operators need to deploy many more 5G small cells in denser environments. This R&D involves the development of analog, hybrid and digital beamforming systems and their relative feasibility. This article discusses these methods and concludes an all-digital antenna approach leveraging digital beamforming is the best and inevitable architecture.

BEAMFORMING AND MIMO

Beamforming is the manipulation of an antenna pattern to control the mainlobe and sidelobe responses. A variety of methods can be used to accomplish this, though the dominant method discussed in this article is with multi-element antennas with phase control or delay. At a certain carrier frequency and with a properly designed multi-element antenna, a phase shift calculated for each antenna element can change or “steer” the

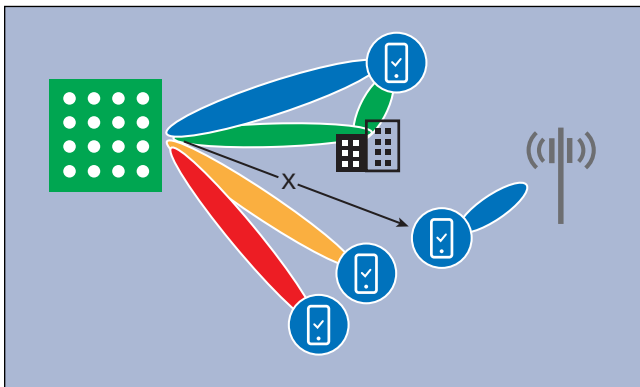
antenna pattern. Beam steering with phase shifts can be used with linear antenna arrays to change the azimuth antenna pattern, and 2D antenna arrays can control the pattern in both azimuth and elevation.

Beamforming benefits mmWave communications since mmWave antenna systems typically have narrow antenna patterns with high attenuation, and multi-element antennas with active beamforming can increase the gain of the aperture and steer the beam toward a desired target to achieve the maximum signal quality. With sufficiently sophisticated beam steering technology, active beam steering enables a mmWave communications link to have a longer range and greater throughput.

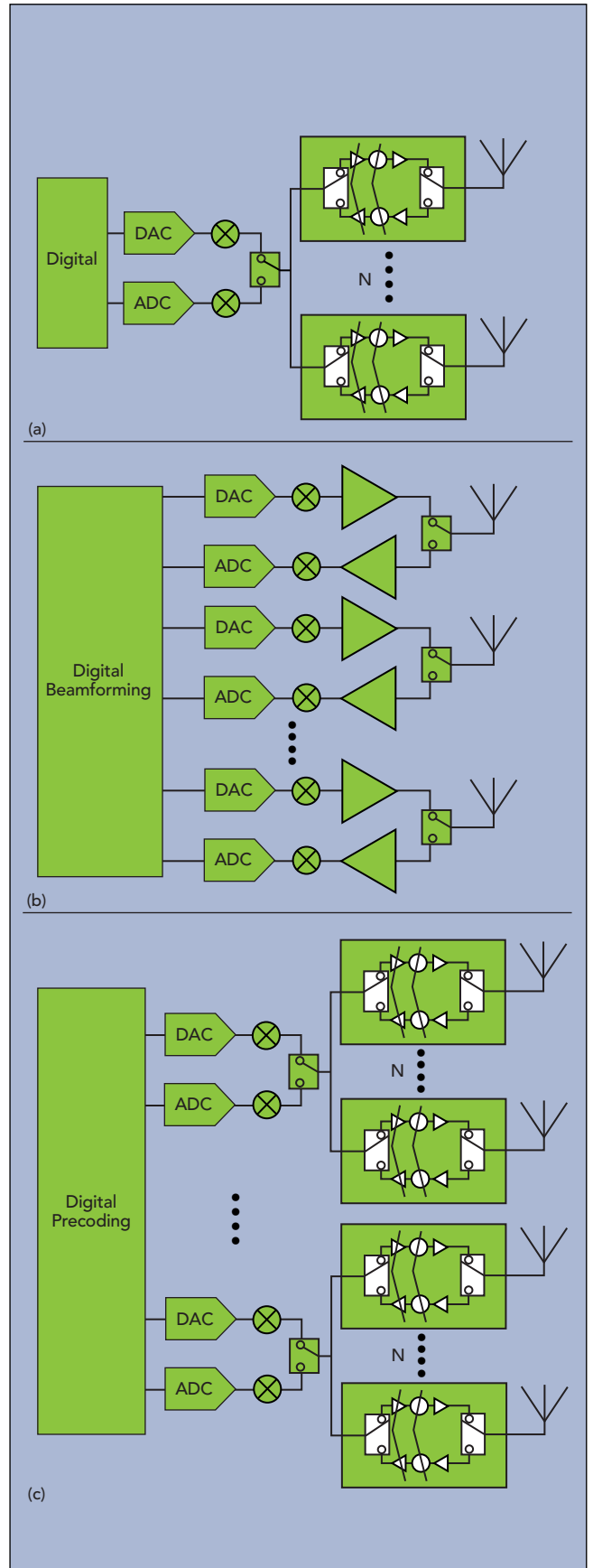
A related topic is using spatial diversity with multi-element antennas to create more than one signal path from a given antenna array to the user, a method known as MIMO (see **Figure 1**). The ability to transmit and receive multiple spatial streams allows for additional communication to occur simultaneously, either augmenting the throughput to a single user (SU-MIMO) or multiple users (MU-MIMO). Employing MIMO technology is another method to enhance the throughput of 5G communications and connect larger numbers of users simultaneously, without deploying additional cells. These techniques generally best serve dense urban environments and require multiple radio channels. In the case of mmWave, extremely narrow beamwidths, high atmospheric attenuation and the likelihood that multipath and reflections will suffer from high attenuation limit the potential gains for MIMO technology.

BEAMFORMING TYPES

The original analog beamforming antenna systems used fixed delays created by phase shifters at each antenna element to create a static beam pattern designed for a single frequency. Advancements of this approach added switches to select among several fixed phase shifters, creating a set of pre-designated antenna patterns. Further advancements adopted adjustable phase shifters at each antenna element, enabling a flexible, actively controlled phased array antenna, i.e., AESAs. With these beamforming antennas, the digital signals are usually created at baseband using digital-to-analog



▲ Fig. 1 MIMO can increase capacity and coverage in dense urban and in-building environments by pointing beams and creating nulls. Source: Ericsson.¹²



▲ Fig. 2 Simplified block diagrams of analog (a), digital (b) and hybrid beamforming (c). Source: Analog Devices.⁸

converters (DAC), converted to RF via frequency conversion and split to feed the transmit/receive (T/R) modules with phase shifters at each element. The received signal follows the reverse path; after down-conversion, the RF is digitized with an analog-to-digital converter (ADC) for processing. The T/R module contains the phase shifter, amplitude control and power and low noise amplifiers. This architecture, known as analog beamforming, requires a separate control signal for each phase shifter at each of the antenna elements and is limited to steering a single spatial beam (see **Figure 2a**).

A more recent approach uses DACs and ADCs directly connected to each T/R module. This method, known as elemental digital beamforming, enables the beamforming algorithms and digital baseband processing to be entirely implemented with robust digital hardware, eliminating the need for sensitive analog RF phase shifters used with analog beamforming. Digital processing is capable of creating multiple spatial streams simultaneously, such that a single antenna array can dynamically create MIMO data streams and beams optimized in real-time for the user and load requirements (see **Figure 2b**).

The biggest challenge for digital beamforming is power consumption. Analog beamforming requires lower DC power. However, since each analog beamformer only supports a single beam—and a digital beamformer enables multiple concurrent beams—digital beamforming is favored in high density environments demanding low latency and uncongested communication. Digital beamforming is particularly attractive for infrastructure networks supporting mobile users.

As the data conversion requirements of elemental digital beamforming systems are the bottleneck for provisioning digital beamforming solutions, cost and power considerations for mmWave antenna arrays have led to an interim approach using hybrid beamforming. Although there are various methods, hybrid beamforming generally combines the analog beamforming phase shifting topology for a subset of the antenna elements—with RF phase shifters, attenuators, low noise and power amplifiers, switching and circulators/isolators still used—and each subarray is driven by data converters with some level of digital precoding (see **Figure 2c**). With this approach, the processing load on the digital electronics and power consumption are less than with elemental digital beamforming. Hybrid beamforming typologies can be designed to allow for multiple spatial streams, although it is less flexible than elemental digital beamforming since the number of beams is limited to the number of hybrid subsets.

To realize elemental digital beamforming for mmWave multi-element antennas, the electronics must be capable of processing Gbps of throughput in real-time, while minimizing latency. 5G, for example, requires signal bandwidths up to 400 MHz. Elemental or all-digital beamforming requires that modulation, demodulation, conversion, spatial processing and beamforming processing occur in real-time, or at least fast enough to track a mobile user. Therefore, more intelligence is required with all-digital beamforming antennas than just baseband processing and beamforming, and these added digital functions are energy expensive. If realized as a discrete

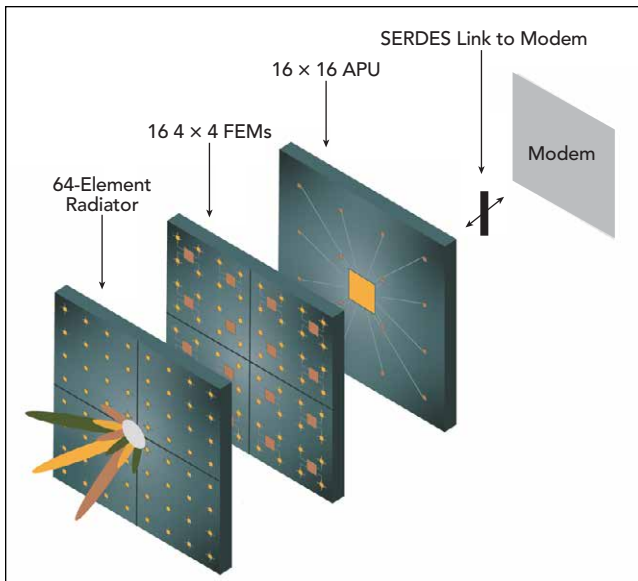
module, they add significant complexity to the physical layout, increasing size and, likely, cost. This is especially true if software-defined logic, such as FPGAs, is used. At this point, thermal management and power management become significant design considerations and high density and high throughput board-to-board and cable-to-board interconnects may be required. To avoid this complexity, a fully integrated ASIC with multi-channel wide bandwidth data conversion and efficient FinFET CMOS digital processing is required to meet the promise of digital beamforming. IQ-Analog has defined a family of APUs to service this emerging market need.

While an analog beamforming antenna system is less complicated and is generally more power efficient than comparable hybrid or digital beamforming antennas, the size and cost of discrete analog components and interconnects pose complexity issues as the antenna array grows beyond a small size. For antenna arrays greater than 4×4 or 8×8 , hybrid beamforming or digital beamforming offer size, weight and cost advantages. Operators typically desire minimal changes to the form factor and power of their equipment, to keep leasing and operational costs down. While 5G mobile handsets can operate with roughly the same data and power efficiency as with 4G, 5G mmWave antenna infrastructure must be deployed at roughly $10\times$ greater density and deliver $10\times$ greater data capacity, which demands the most efficient multi-beam digital antenna processors. The unique digital antenna processing needs of mmWave antennas must be addressed using the most highly integrated and streamlined methods possible, meaning a unique ASIC composed of high channel count data converters, digital antenna processing and high speed digital I/O systems.

ALL-DIGITAL ANTENNAS

With greater component integration, the hybrid and digital topologies become more feasible, enabling mmWave beamforming and MIMO antennas to have a greater number of antenna elements. This shift enables more capable and flexible antenna systems that can provide higher gain with SU-MIMO or MU-MIMO operation. The promise of these architectures hinges on the performance of the digital and conversion electronics, i.e., the ability of the direct RF sampling and direct digital synthesis to address the full capacity of the mmWave spectrum. Otherwise, additional frequency translation hardware will be required, increasing complexity and reducing flexibility.

These trade-offs materialize as modem and beamforming technologies designed strictly for a single application, which may be infeasible for commercial and military manufacturers who want more flexible and capable solutions to support complex licensing and geographic restrictions. Direct RF sampling enables more flexible use of spectrum and does not limit a mmWave antenna to set 28 or 39 GHz frequency bands; any spectrum within the capability of the RF sampling hardware is accessible. Direct RF sampling is ideal when paired with software-defined radios (SDR); however, it presents a challenge for the data converters to meet the performance requirements.



▲ Fig. 3 mmWave all-digital antenna.

With the specifications for mmWave 5G and tactical communications not fully defined and likely to change, the trend is for modem suppliers to provide SDR solutions rather than fixed modems. As the mmWave standards evolve, the SDR can be reprogrammed to meet the updated standard, whether for 5G or military applications. Modular scalability at the antenna elements and beamforming hardware is desirable for mmWave 5G base stations, to provide the flexibility to be upgraded without complete and costly hardware replacement. This is critical for operators, as the number of 5G mmWave base stations will be roughly 10× the number of 4G base stations to provide similar coverage. The number of 5G mmWave base stations may actually reach the same order of magnitude as mobile 5G handsets.

To take full advantage of SDR technology, full spectrum conversion and digital beamforming APUs are needed, an architecture dubbed all-digital antennas. The all-digital antenna, a digital beamforming phased array that supports several wide bandwidth MIMO beams, integrates an antenna array, RF front-end (RFFE) SoC and multi-chip module containing an APU and modem using a high speed converter interface, such as JESD204B (see **Figure 3**).¹³ The APU contains digital down-conversion with decimation and up-conversion with interpolation. Ideally, the all-digital antenna beamforming function is an ASIC rather than an FPGA or FPGA-ASIC hybrid. Though feasible in each configuration, building an FPGA-based all-digital antenna requires a greater footprint and significantly higher power consumption, with greater latency and likely higher cost. The best configuration would be a monolithic FinFET ASIC, with the most efficient data converter and digital processing.

CONCLUSION

Though the trend toward integration and all-in-one ICs was a slow process for prior generations of wireless communications (i.e., 2G, 3G, 4G and Wi-Fi), the path

toward ASIC-based APUs and a more efficient all-digital antenna for 5G will be accelerated by 5G's tremendous market demand. High performance full spectrum conversion APUs have already been fabricated in FinFET CMOS, and the underlying technology exists to realize multi-channel APU derivatives capable of the several GHz of addressable signal bandwidth needed for 5G. Designed with flexibility and programmability, these APUs can be readily adapted to a range of mmWave applications, such as 5G, tactical communications, autonomous vehicle radar and V2X and LEO SATCOM.n

References

1. "mmWave for Army Tactical Communications," *SBIR Funding Topic*, November 2018, www.sbir.gov/sbirsearch/detail/1531631.
2. S. Carlson, "Raytheon Tapped by DARPA for High Frequency Digital Communications Research," *UPI*, November 6, 2018, www.upi.com/Raytheon-tapped-by-DARPA-for-high-frequency-digital-communications-research/3351541528087/.
3. "Military Communications Market: Technological Advancements & Propelling Demand for C4ISR Systems to Drive Growth in Developing Markets: Global Industry Analysis (2013-2017) and Opportunity Assessment (2018-2028)," *Future Market Insights*, June 2018, www.futuremarketinsights.com/reports/military-communications-market.
4. "Millimeter-Wave Beamforming: Antenna Array Design Choices & Characterization," *Rohde & Schwarz*, https://scdn.rohde-schwarz.com/ur/pws/dl_downloads/dl_application/application_notes/1ma276/1MA276_2e_Beamform_mmW_AntArr.pdf.
5. T. S. Rappaport et al., "Overview of Millimeter Wave Communications for 5G Wireless Networks-with a focus on Propagation Models," *IEEE Transactions on Antennas and Propagation*, November 2017.
6. "The Military Communications Market: 2015-2030—Opportunities, Challenges, Strategies & Forecasts," *HTF Market Intelligence*, April 2015, www.htfmarketreport.com/reports/17351-the-military-communications-market.
7. C. Scarborough et al., "Beamforming in Millimeter Wave Systems: Prototyping and Measurement Results," *2018 IEEE 88th Vehicular Technology Conference*, August 2018.
8. T. Cameron, "Bits to Beams: RF Technology Evolution for 5G Millimeter Wave Radios," *Analog Devices*, www.analog.com/media/en/technical-documentation/tech-articles/Bits-to-Beams-RF-Technology-Evolution-for-5G-mmwave-Radios.pdf.
9. P. Sagazio et al., "Architecture and Circuit Choices for 5G Millimeter-Wave Beamforming Transceivers," *IEEE Communications Magazine*, Vol. 56, No. 12, December 2018.
10. J. Zhang et al., "5G Millimeter-Wave Antenna Array: Design and Challenges," *IEEE Wireless Communications*, Vol. 24, No. 2, April 2017.
11. A. H. Naqvi and S. Lim, "Review of Recent Phased Arrays for Millimeter-Wave Wireless Communication," *Sensors*, September 21, 2018, www.ncbi.nlm.nih.gov/pmc/articles/PMC6211090/.
12. P. von Butovitsch et al., "Advanced Antenna Systems for 5G Networks," *Ericsson*, www.ericsson.com/en/white-papers/advanced-antenna-systems-for-5g-networks.
13. "ADI JESD204B Survival Guide," *Analog Devices*, www.analog.com/media/en/technical-documentation/technical-articles/JESD204B-Survival-Guide.pdf.

Exploring Hybrid Beamforming Architectures for Massive MIMO 5G Systems

MathWorks

The 5G goals of higher data rates, lower-latency network access, and more energy-efficient implementation are clear. Higher data rates drive the need for greater-bandwidth systems. The available bandwidth in the spectrum up through 6 GHz is not sufficient to satisfy these requirements, so the next generation of wireless communication systems are targeting operating frequency bands in the millimeter wave range.

INTELLIGENT ARRAY DESIGN WITH BEAMFORMING

Smaller wavelengths at these higher-frequency bands enable implementations with more antenna elements per system within small form factors. Signal path and propagation challenges associated with operating at these frequencies also increases. You can offset these losses with intelligent array design and the use of spatial signal processing techniques, including beamforming. This type of processing is enabled by massive MIMO arrays and can be used directly to provide higher link-level gains to overcome path loss and undesirable interference sources.

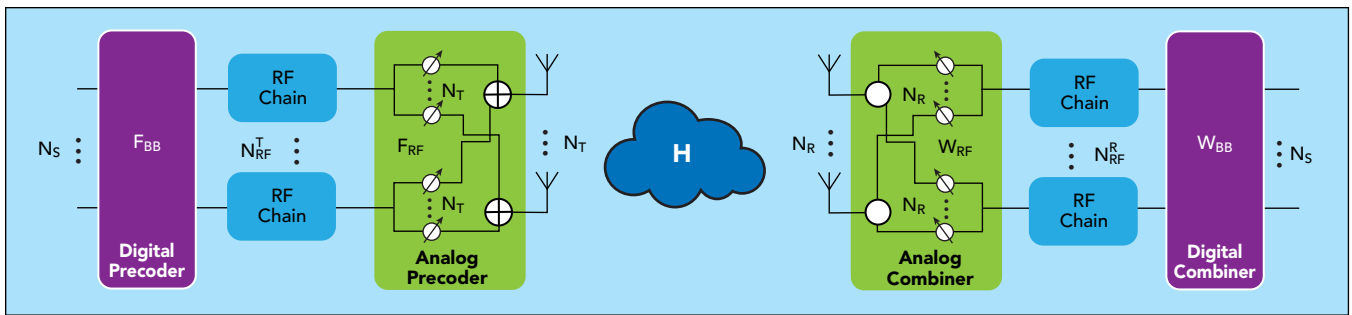
Having independent weighting control over each antenna array element provides you with the most control and flexibility with beamforming in an active array design. This approach requires a transmit/receive (T/R) module dedicated to each element. For array sizes that

are typical of a massive MIMO communication system, this type of architecture is difficult to build due to cost, space, and power limitations. For example, having a high-performance ADC/DAC or power amplifier for every channel can drive the cost and power beyond allocated design budgets.

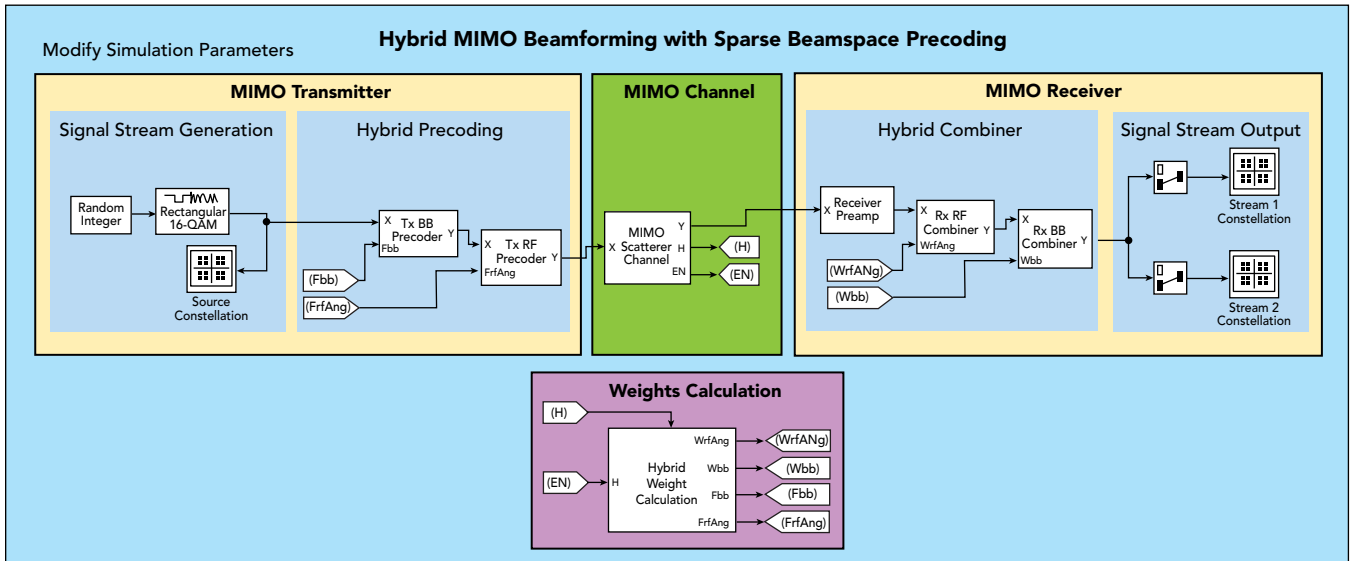
[5G New Radio \(NR\)](#) wireless communication systems use [MIMO beamforming](#) technology for signal-to-noise ratio (SNR) enhancement and spatial multiplexing to improve the data throughput in scatterer-rich environments. In a scatterer-rich environment, line-of-sight (LOS) paths between the transmit and receive antennas are not always present.

To gain the required throughput, MIMO beamforming implements precoding on the transmitter side and combining on the receiver side to increase SNR and to separate spatial channels. A full digital beamforming structure requires each antenna to have a dedicated RF-to-baseband chain, which can increase the overall hardware cost and drive the power consumption higher.

Hybrid beamforming is a technique for partitioning beamforming operations between the digital and RF domains to employ fewer RF-to-baseband chains. With deliberate selection of the weights for precoding and combining, hybrid beamforming can achieve a level of performance that approaches that of full (all-digital) beamforming.



▲ Fig. 1 Hybrid beamforming system structure: transmitter, channel, and receiver. © 1984–2019 The MathWorks, Inc.



▲ Fig. 2 Behavioral model of a hybrid beamforming system. © 1984–2019 The MathWorks, Inc.

Hybrid beamforming designs are developed by combining multiple array elements into subarray modules. A T/R module is dedicated to a subarray in the array, so fewer T/R modules are required in the system. The number of elements, and the positioning within each subarray, can be selected to ensure system-level performance is met across a range of steering angles.

Each element within a subarray can have a phase shift applied directly in the RF domain, while digital beamforming techniques based on complex weighting vectors can be applied on the signals that feed each subarray. Digital beamforming allows control of the signal for both amplitude and phase on signals aggregated at the subarray level. For cost and complexity reasons, the RF control is typically limited to applying phase shifts to each of the elements.

Hybrid beamforming systems are complex to develop. You can use modeling techniques to design and evaluate massive MIMO arrays and the corresponding RF and digital architectures needed to help manage their complexity. With these techniques, you can reduce risk and validate design approaches at the earliest stages of a project. Baseband equivalent models can be used for initial insight. These models can be developed quickly, and they provide the fastest simulation speed options. Subsystems can be integrated to form a physical layer simulation. The resulting model can be used to drive partitioning decisions between the RF and digital domains.

DEFINITION OF PARAMETERS SHOWN IN FIGURE 1

F_{RF}	Analog precoder of size $N_T \times N_{RF}^T$	N_T Number of Tx antennas
F_{BB}	Digital precoder of size $N_{RF}^T \times N_S$	N_R Number of Rx antennas
W_{RF}	Analog combiner of size $N_R \times N_{RF}^R$	N_S Number of signal streams
W_{BB}	Digital combiner of size $N_{RF}^R \times N_S$	N_{RF}^T Number of Tx RF chains
H	MIMO channel matrix of size $N_R \times N_T$	N_{RF}^T Number of Rx RF chains

The scattering channel is denoted by H .

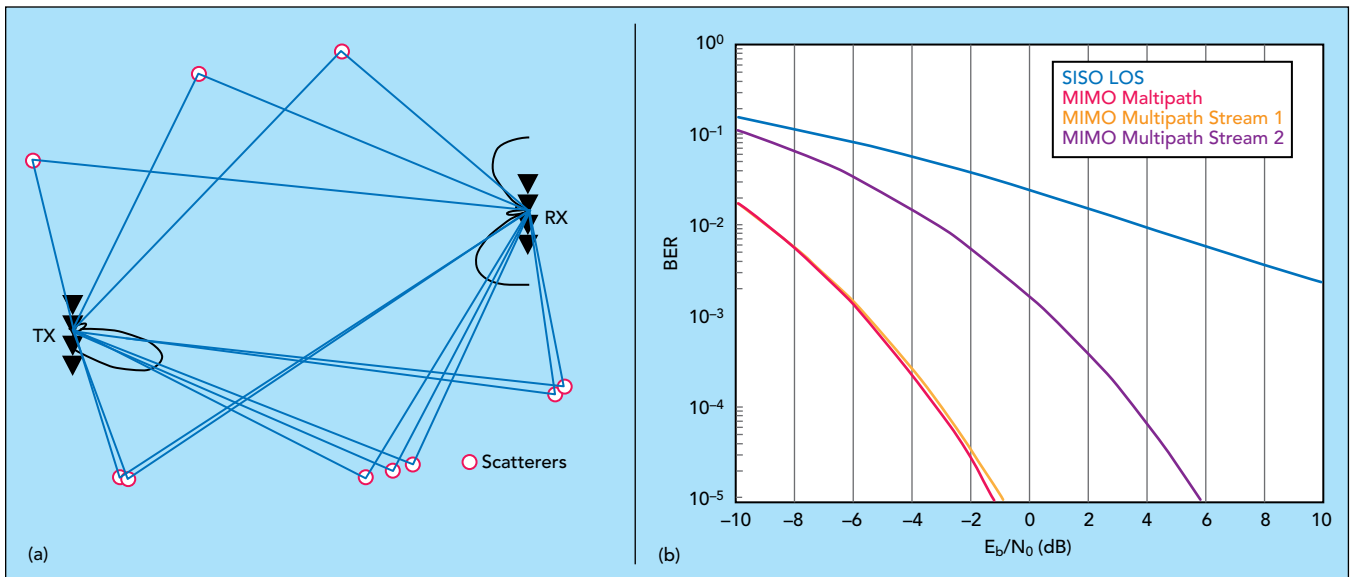
HYBRID BEAMFORMING ARCHITECTURE

Figure 1 shows a block diagram of a hybrid beamforming system with a transmitter, a channel, and a receiver.

BUILDING THE MODEL

The challenge in developing a massive MIMO system is reducing hardware without reducing system performance.

Using a behavioral model helps you explore different parameter values such as the number of antennas and



▲ Fig. 3 Multiscatterer scenario (left) and BER in multipath scenarios vs. LOS (right). © 1984–2019 The MathWorks, Inc.

the number of RF chains. The number of RF chains is important because this is where hardware cost savings can be achieved. By “sharing” the digital weights across multiple RF channels, less hardware is needed. Using a behavioral model, hybrid beamforming algorithms can be developed and tested before system implementation. You can also generate both the RF phase shifts and digital weights directly for each configuration.

The model of the system consists of the following four major components, as shown in **Figure 2**:

- MIMO transmitter
- MIMO channel
- MIMO receiver
- Hybrid weight calculation

The structures of the transmitter, receiver, and MIMO channel blocks are independent from the precoding and weight matrix generation. The model includes a weight calculation block that implements different beamforming algorithms and can be customized.

A MIMO channel matrix H can be estimated in the transmitter or receiver, depending on the time or frequency division duplexing (TDD or FDD) modes used. The channel matrix H is invariant to the number of transmitted symbols, so the precoding and combiner matrices will be the same for all symbols.

The MIMO transmitter generates the signal stream and then applies the precoding to leverage spatial multiplexing. The modulated signal is propagated through a scattering channel defined in the MIMO channel and then decoded and demodulated at the receiver side.

WHY SPATIAL MULTIPLEXING?

To achieve the higher channel capacity needed for 5G, the system must operate in multipath fading environments. A MIMO system with spatial multiplexing can send multiple data streams simultaneously across a multipath channel and a rich scattering environment in order to increase the information throughput.

With [spatial multiplexing](#), the channel matrix is separated into multiple modes so that data streams sent

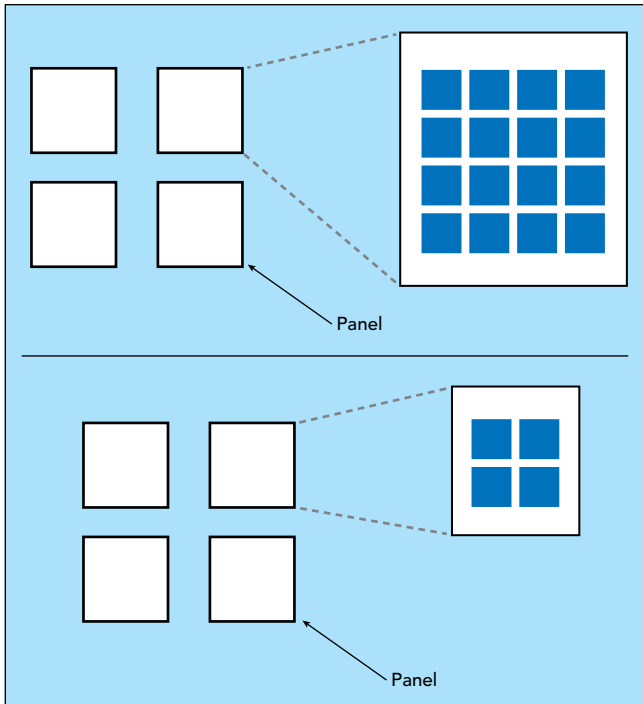
from different elements in the transmit array can be independently recovered from the received signal. To achieve this result, each data stream is precoded before the transmission and then combined and recovered after the reception. The information collected by each receiver element is simply a scaled version of the signal at each transmit array element, which means it behaves like multiple orthogonal subchannels within the original channel. The first subchannel corresponds to the dominant transmit and receive directions, but signal processing techniques can be used to equalize the subchannels. In addition, it is possible to use other subchannels to carry information. Intelligence can be applied to the allocated power per element; industry research is still very much active in this area.

With this backdrop, the next question is, how do your array design choices impact your system-level performance? The answer really depends on the nature of the channel. Arrays can be used to either improve the SNR via the array gain or the diversity gain, or improve the capacity via the spatial multiplexing.

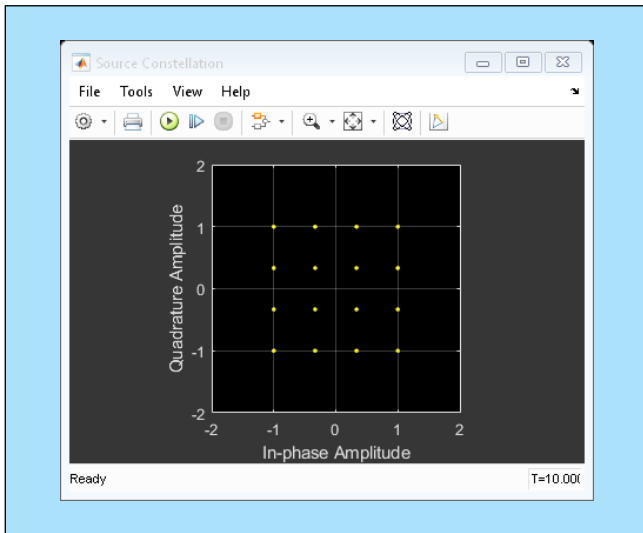
Figure 3 illustrates an abstracted view of a multiscatterer channel. Also, in **Figure 3**, you can see the throughput for a single LOS data stream compared with that of multiple data streams (two in this case) in a multipath environment. Note that although the second stream doesn't provide a gain as high as the first stream (because it uses a less dominant subchannel), the overall information throughput is improved. Again, equalization techniques can be applied to improve the nondominant channels. This concept can easily extend to many more channels.

MIMO TRANSMITTER AND RECEIVER

For the transmitter and receiver subsystems, the focus of the engineering tradeoff is cost vs. performance. This tradeoff drives partitioning of the [beamforming architecture](#) between the RF and baseband domains. Partitioning in turn brings us to the topic of subarrays, in which multiple antenna elements are mapped to spe-



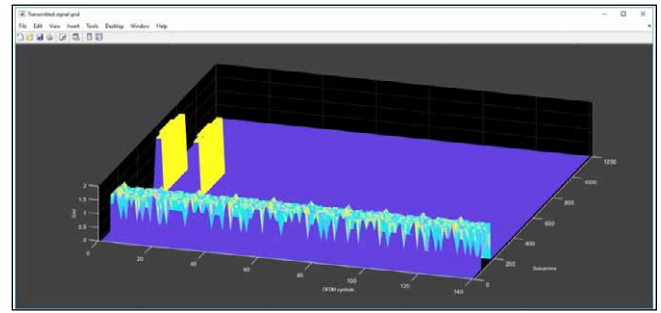
▲ Fig. 4 64-element transmit array with four RF chains (top), and 16-element receive array with four RF chains (bottom). © 1984–2019 The MathWorks, Inc.



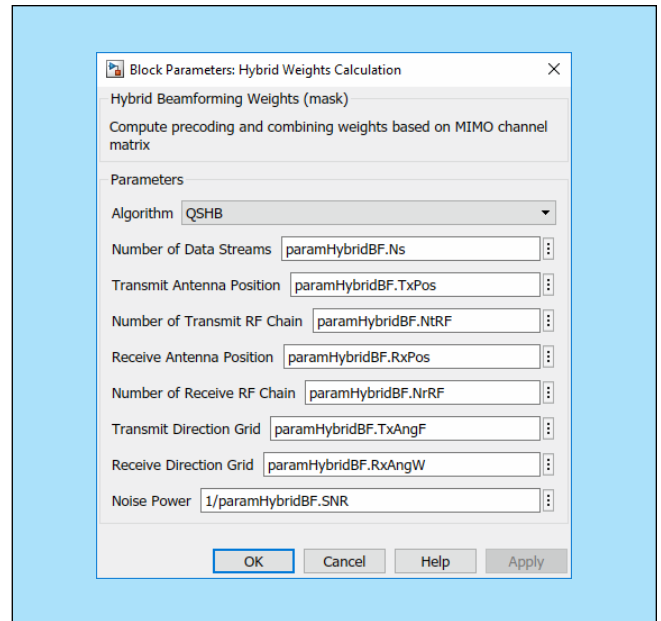
▲ Fig. 5 Constellation diagram of 16-QAM modulation. © 1984–2019 The MathWorks, Inc

cific RF channels. Subarrays are integrated to build up a full antenna array. Sometimes element feeds are shared across subarrays to create virtual arrays. In this scenario, the total number of transmit/receive modules is lower than the number of antenna elements for each subarray, which results in less hardware in large systems.

Having less hardware is an advantage from a cost and power perspective, but without an all-digital beamforming design, some flexibility is sacrificed in the RF portion of the beam steering. This occurs when the same RF phase shift value is applied to each channel of a subarray. It contrasts with the all-digital case, in which phase and amplitude weighting can be unique values for each channel.



▲ Fig. 6 5G New Radio downlink waveform. © 1984–2019 The MathWorks, Inc.



▲ Fig. 7 Hybrid weight mask to compute precoding and combining weights based on a MIMO channel matrix. © 1984–2019 The MathWorks, Inc.

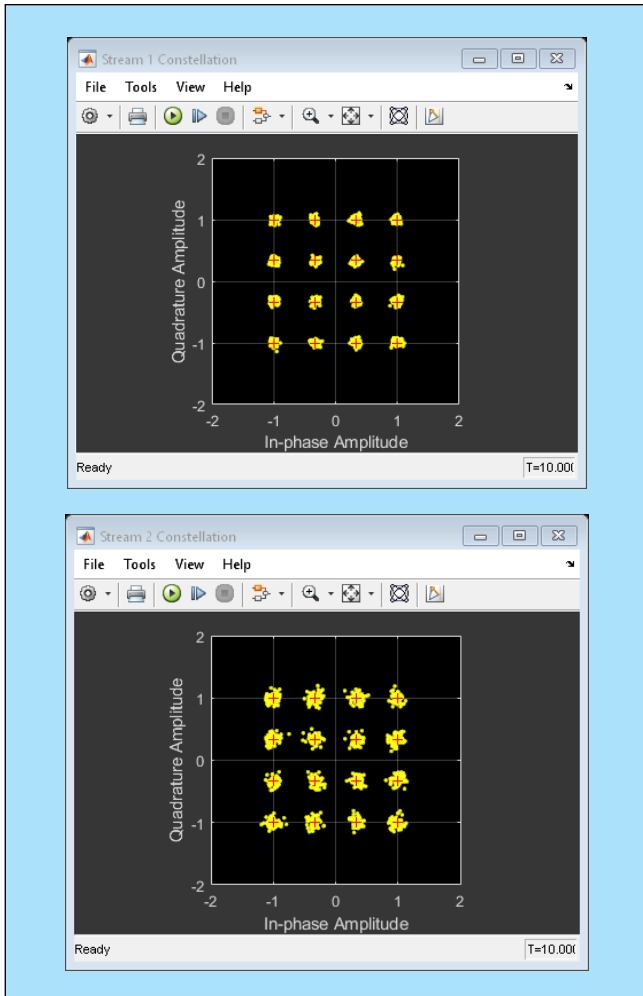
In this example, two signal streams are generated. The transmitter system consists of 64 transmit antennas with four transmit RF chains. There are 16 receive antennas that feed four RF chains. Both arrays are shown in **Figure 4**.

It is also desirable to improve channel capacity by maximizing the spectral efficiency. One way this could be accomplished is to require that each RF chain be used to send an independent data stream. Assuming the channel is known, the unconstrained optimal precoding weights can be obtained by diagonalizing the channel matrix and extracting the dominant modes.

WAVEFORM GENERATION

For simplicity, this example model uses a 16 QAM modulation scheme. The constellation diagram for this modulation scheme is shown in **Figure 5**.

However, the model can accommodate a range of modulation schemes, including 5G-compliant [uplink](#) and [downlink](#) waveforms. These waveforms are defined by parameters including synchronization signal definition, carrier configuration, and control resource set. Multiple bandwidth parts (BWPs) may also be required. A BWP is formed by a set of contiguous resources shar-



▲ Fig. 8 Stream 1 and 2 constellation diagrams for QSHB. © 1984–2019 The MathWorks, Inc.

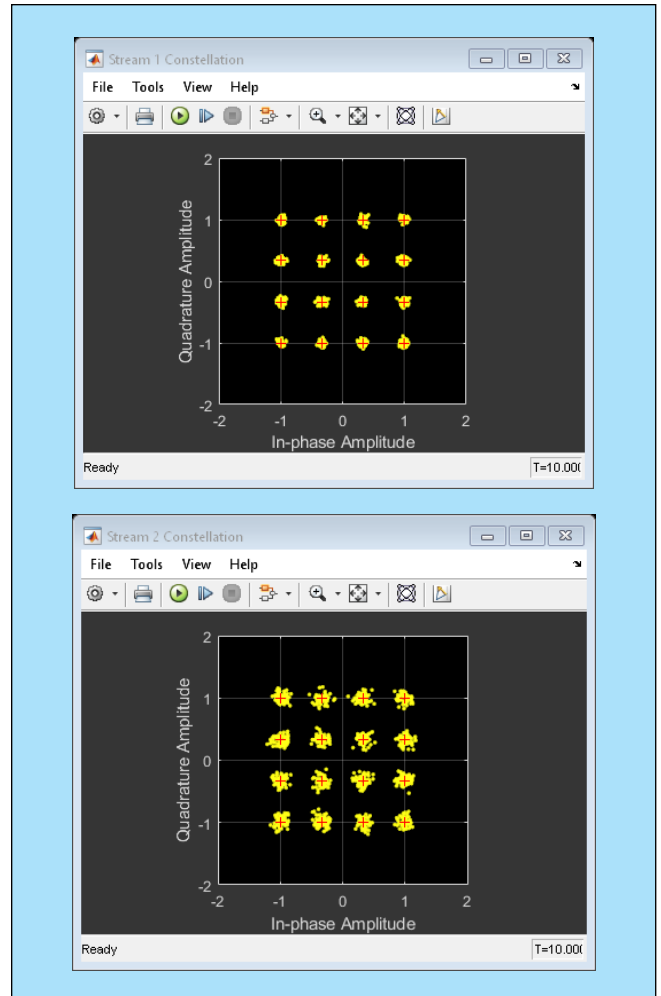
ing a numerology on a given carrier. Each BWP can have different subcarrier spacings (SCSs), use different cyclic prefix (CP) lengths, and span different bandwidths.

Figure 6 shows an example waveform as a function of subcarriers and symbols.

HYBRID BEAMFORMING WEIGHTS COMPUTATION

In a hybrid beamforming system, both the precoding and the corresponding combining process are performed across baseband and RF. In general, the beamforming achieved in RF involves phase shifts. Therefore, a critical component of the workflow is to determine how to distribute the weights between the baseband and the RF band based on the channel. The system model provides a framework for analyzing alternative weight distribution architectures.

The precoding weights, F_{bb} and F_{rfAng} , and combining weights, W_{bb} and W_{rfAng} , are computed based on the channel matrix, H . **Figure 7** shows the block parameters that are used to compute both the precoding and combining weights for the MIMO channel. These can be configured to explore other system combinations.



▲ Fig. 9 Stream 1 and 2 constellation diagrams for HBPS. © 1984–2019 The MathWorks, Inc.

QUANTIZED SPARSE HYBRID BEAMFORMING

You can recover the 16-QAM symbol streams at the receiver using the quantized sparse hybrid beamforming (QSHB) algorithm. The resulting constellation diagram (see **Figure 8**) shows that compared with the source constellation, the recovered symbols are properly located in both streams. This result demonstrates that by using the hybrid beamforming technique, you can improve the system capacity by sending the two streams simultaneously. In addition, the constellation diagram shows that the variance of the first recovered stream is better than that of the second recovered stream as the points are less dispersed. This is because the first stream uses the most dominant mode of the MIMO channel, so it has the best SNR.

Using a QSHB algorithm produces the analog precoding and combining weights, which are just steering vectors corresponding to the dominant modes of the channel matrix H of a MIMO scattering channel:

- Precoding matrices F_{RF} and F_{BB}
- Combining matrices W_{RF} and W_{BB}

Having the resolved hybrid beamforming matrices, the estimates \hat{s} of the N_s signal streams can be represented as:

$\hat{\mathbf{s}} = \sqrt{\rho} \mathbf{W}_{\text{BB}}^* \mathbf{W}_{\text{RF}}^* \mathbf{H} \mathbf{F}_{\text{RF}} \mathbf{F}_{\text{BB}} \mathbf{s} + \mathbf{W}_{\text{BB}}^* \mathbf{W}_{\text{RF}}^* \mathbf{n}$
 where \mathbf{s} is the signal stream of dimension N_s and \mathbf{n} is the channel noise vector of dimension N_R .

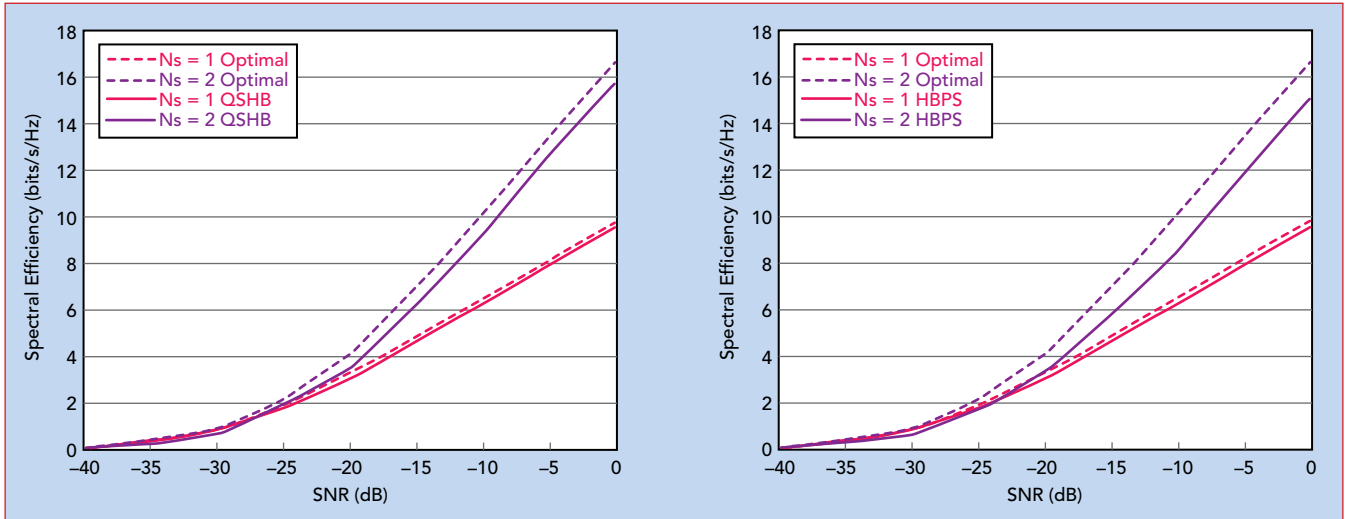
QUANTIZED SPARSE HYBRID BEAMFORMING WITH PEAK SEARCH

Quantized sparse hybrid beamforming with peak search (HBPS) is a simplified version of QSHB. Instead of searching for the dominant mode of the channel matrix iteratively, HBPS projects all the digital weights into a grid of directions and identifies the N_{RF}^T and N_{RF}^R

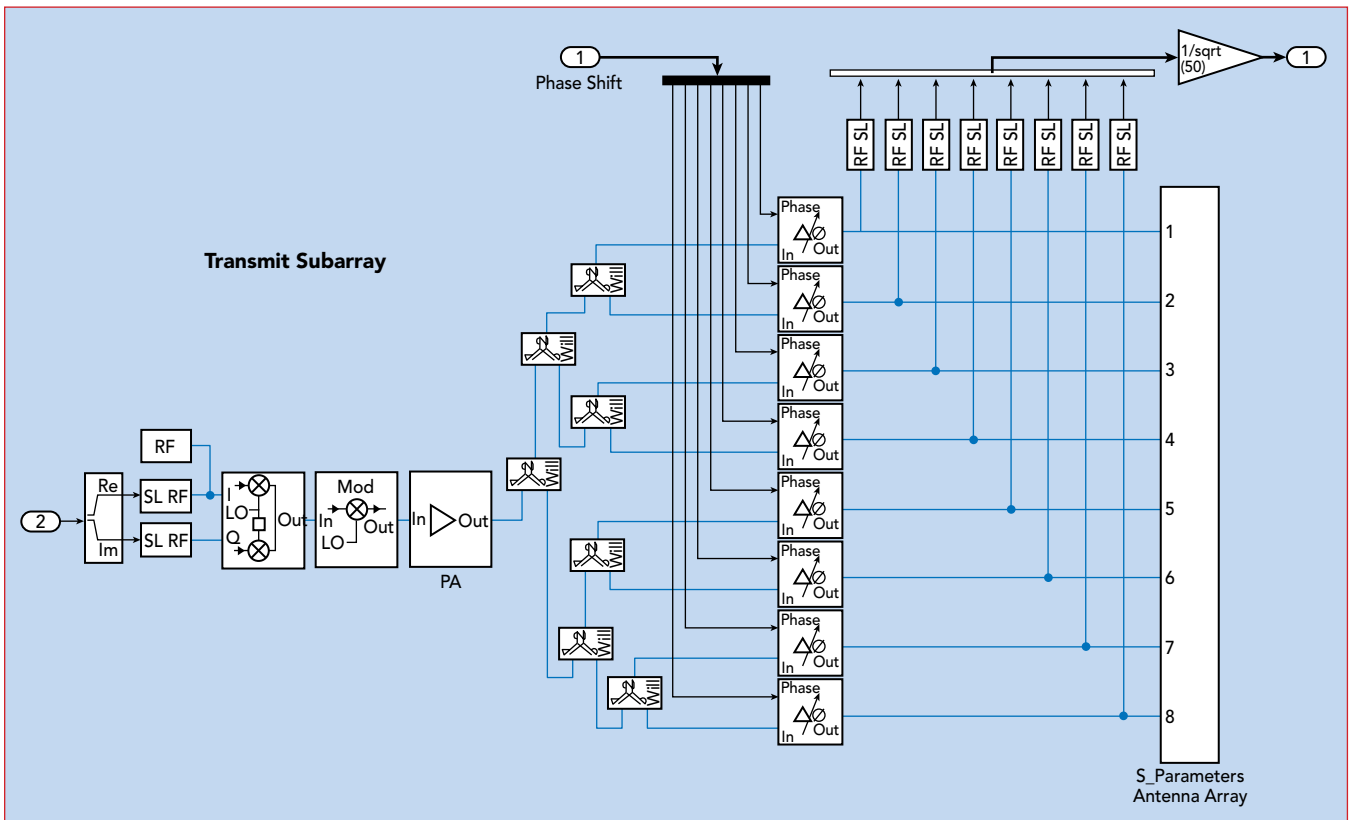
peaks to form the corresponding analog beamforming weights. This works well, especially for large arrays, like the ones used in massive MIMO systems. This is because for large arrays, the directions are more likely to be orthogonal.

Because the channel matrix can change over time, the weights computation needs to be performed periodically.

The result of HBPS is shown in **Figure 9**. The constellation diagram shows that its performance is similar to that of QSHB. This means that the HBPS is a good choice for the simulated 64×16 MIMO system.



▲ Fig. 10 Efficiency comparison of QSHB (left) and HBPS (right). © 1984–2019 The MathWorks, Inc.



▲ Fig. 11 Example of RF Blockset hybrid structure with baseband and RF weighting. © 1984–2019 The MathWorks, Inc.

SPECTRAL EFFICIENCY COMPARISON OF ALGORITHMS

Spectral efficiency, a common MIMO system performance metric, can be used to measure the effectiveness of the partitioning. You can compare the spectral efficiency achieved using the optimal weights (all-digital weights) using the proposed hybrid beamforming algorithms, QSHB and HBPS.

For ease of understanding, the simulation uses one- and two-signal streams, but this approach can also be extended to match your system. The transmitter antenna array can also be defined to match your system requirements.

For this system, the array pattern covers 80 degrees in azimuth and 40 degrees in elevation, and the receiver antenna covers 120 degrees in azimuth and 80 degrees in elevation. The resulting spectral efficiency curves are obtained from 50 Monte Carlo trials for each SNR value. In the plots in **Figure 10**, the spectral efficiency of QSHB is about 1dB off from the optimal full digital beamforming.

While the HBPS algorithm provides better computational efficiency, an additional loss of up to 1.5 dB in spectral efficiency occurs compared to the QSHB.

EXTENDING THE FIDELITY OF RF AND ANTENNA ARRAY MODELS

With a model of the hybrid beamforming system in place, you can move to higher levels of fidelity with a multidomain simulation of the system. Nonlinear RF amplifiers and model effects can be used to estimate gain, noise, and even-order and odd-order intermodulation distortion. RF models can be characterized using data sheet specifications or measured data, and can be used to accurately simulate adaptive architectures, including automatic gain control (AGC) and digital predistortion (DPD) algorithms.

Modeling RF systems using circuit envelope simulation enables high-fidelity, multicarrier simulation of networks with arbitrary topologies. **Figure 11** shows

an example of a hybrid system with a partitioned system. Here, baseband weighting is applied to the digital streams that feed each transmit/receive module. The remaining weights are applied as phase shifts to the RF channels feeding the antenna elements.

SUMMARY

MIMO arrays and the corresponding RF and digital architectures are critical components of [5G designs](#). These components also drive the related hybrid beamforming systems. A balance must be reached in these systems to meet system performance goals and system-level cost objectives. Modeling and simulation techniques can help reduce the risk associated with this complex workflow. Higher levels of fidelity can be added across the project life cycle to bring the model in line with the end system implementation.

Developing a hybrid beamformer and evaluating algorithm alternatives is only the first step toward achieving the required performance of a wireless communications system. To assess performance, the beamformer must be integrated into a system-level model and evaluated over a collection of parameter, steering, and channel combinations.

Using MATLAB and Simulink, you can design antenna, RF, and signal processing systems in single environment. Modeling can help you define architectures for hybrid beamforming. You can:

- Design massive MIMO antenna arrays, including complex subarray structures
- Partition hybrid beamforming systems intelligently across RF and baseband domains
- Model MIMO wireless communication systems
- Explore architectural choices and tradeoffs
- Evaluate the quality of partitioning design choices

Modeling these [beamforming](#) algorithms in the context of an entire system, including RF, antenna, and signal processing components, can help you verify design choices at the earliest phases of the project and reduce the associated challenges.

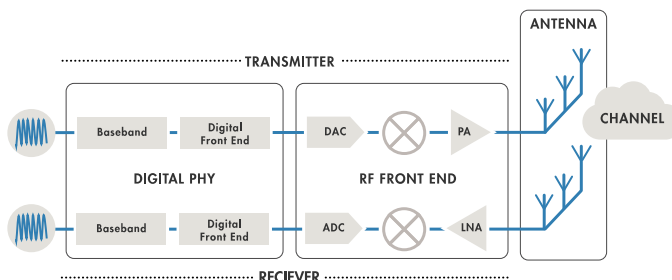


Attending the 2019 European Microwave Conference?

See demos of **MATLAB®** and **Simulink®** for wireless communications

Booth B2155

Register for hands-on workshops: 5G RF, Antenna, Radar, SDR Testing



Adopting the 64 to 71 GHz Band for Fixed Wireless Applications

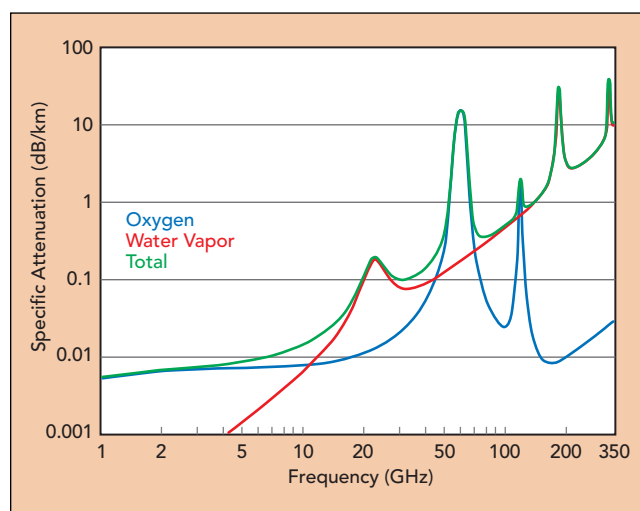
Sivers IMA
Kista, Sweden

The 60 GHz band (57 to 64 GHz) has long been recognized as ideal for dense urban data networks because of its large capacity combined with excellent spectrum reuse, due to oxygen absorption. The use of phased array antenna technology enables novel mesh network architectures and significantly reduces the size and cost of equipment, compared to conventional fixed antenna technology, but its reduced range limits some applications. Recent regulatory decisions have opened up additional spectrum from 64 to 71 GHz. This article explores the absorption characteristics across the newly widened band and discusses the applications enabled by commercial transceiver RFICs covering the expanded frequency range from 57 to 71 GHz.

National regulators, responsible for allocating spectrum to different users, must balance competing commercial and government interests. The frequency allocations that the regulators make are determined by the type of application and its needs, such as bandwidth and propagation. The historic use of the band must also be considered. As spectrum needs are common among nations, and spectrum usage has spillover effects across borders, spectrum allocation is necessarily harmonized at the supra-national level by organizations such as the European Conference of Postal and Telecommunications Administrations (CEPT) and the International Telecommunication Union (ITU).

Bands with impairments—such as high attenuation due to water or oxygen absorption—are typically less useful for traditional communications applications. Therefore, regulators have opened them with the intent to enable new applications. The results are often unexpected and transformational: think of cordless phones in the 900 MHz band and Wi-Fi at 2.4 and 5 GHz. Regulators evaluated the same considerations when they allocated the 60 GHz band for unlicensed use.

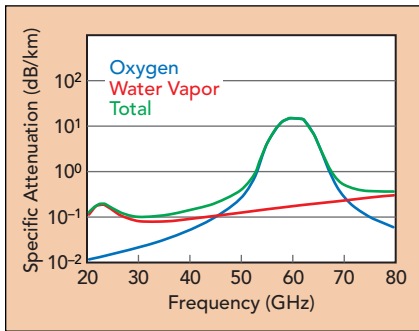
To assist with spectrum allocation, the ITU has published ITU-R P.676-11, "Attenuation by Atmospheric Gases," which estimates the attenuation due to oxygen and water vapor under different conditions and across the frequency range from 1 to 350 GHz (see **Figure 1**). Annex 2 of the recommendation provides a simplified approximate method to estimate gaseous attenuation



▲ **Fig. 1** Specific attenuation vs. frequency from 1 to 350 GHz.

applicable to the full frequency range. The 57 to 64 GHz band coincides with an oxygen absorption peak, which reaches a maximum of approximately 15 dB/km at 60 GHz (see **Figure 2**, which shows more detail). The attenuation in this band is substantially greater than observed for other bands in the low mmWave part of the spectrum, which makes it ideal for short-range applications.

The Federal Communications Commission (FCC) allocated the band from 59 to 64 GHz for unlicensed use in 1995. In 2001, the FCC added spectrum from 57 to 59 GHz, providing a total of 7 GHz for unlicensed use. In

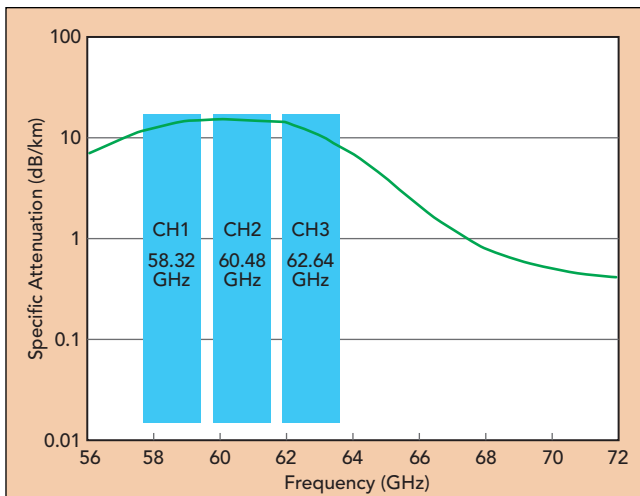


▲ Fig. 2 Specific attenuation from 20 to 80 GHz.

2009, CEPT/ECC/ Recommendation (09)01, "Use of the 57 to 64 GHz Frequency Band for Point-to-Point Fixed Wireless Systems," allocated the same band for unlicensed use, subject to implementation by the national regulators of the 48 CEPT member states.

CHARACTERISTICS OF THE 57 TO 64 GHz BAND

Allocating a substantial contiguous band enables it to be divided into multiple wide channels, which provides for very high data capacity. For example, by using the IEEE 802.11ad channelization, which divides the band into channels of 2.16 GHz with an occupied bandwidth of 1.76 GHz, bit rates up to 4.62 Gbps using 16-QAM single carrier modulation and 8.085 Gbps using 64-QAM single carrier modulation can be achieved. As noted, the 57 to 64 GHz band coincides with the oxygen absorption peak, with a maximum of approximately 15



▲ Fig. 3 Specific attenuation in IEEE 802.11ad channels 1 to 3.

TABLE 1

LINK DISTANCE FOR A 16 Tx, 16 Rx TRANSCEIVER ON IEEE 802.11ad CHANNEL 2

		Modulation and Coding		
	Units	MCS 8 QPSK	MCS 12 16-QAM	MCS 12.3 64-QAM
Maximum Average EIRP	dBm	40	40	37
Nominal Sensitivity	dBm	-89	-82	-77
System Gain	dB	129	122	114
Distance (Ch 2)	m	400	260	135
Distance (Ch 2), No Rain	m	460	290	150

dB per kilometer at 60 GHz. **Figure 3** overlays the atmospheric attenuation for 802.11ad channels 1 through 3, showing the attenuation peaks in channel 2. Channels 1 and 3 experience similar attenuation, meaning the impact on link range is broadly the same for all three channels.

The maximum distance for a radio link to be reliably operated is defined as the point where the system gain—the transmit power measured as EIRP minus the nominal receiver sensitivity—equals the loss from atmospheric attenuation plus effects such as the absorption by rain or reflections from the ground, buildings or other objects. For this analysis, assume rain losses for rain zone K (e.g., Chicago, Beijing or New Delhi) and availability of 99.9 percent, per ITU recommendation ITU-R PN.837-1, "Characteristics of Precipitation for Propagation Modeling."

For phased array implementations, the maximum average EIRP is typically limited by regulation to 40 dBm. The receiver's sensitivity is derived from the per-element sensitivity and the gain of the antenna array. In this example, an array of 16 receive (Rx) elements is modeled, using the performance of a commercially available transceiver RFIC (see **Sidebar**, pg. 15) connected to antennas with a per-element gain of 11 dBi. In principle, RF transceiver ICs can be tiled for greater performance; however, as the transmit power often reaches the regulatory cap, the benefit of tiling is mainly in receiver sensitivity. For a link operating in channel 2, the maximum link distance with a single transceiver using various modulation and coding schemes (MCS) is shown in **Table 1**. The high specific attenuation in these channels yields relatively short link distances, especially at the higher bit rates requiring higher order modulation.

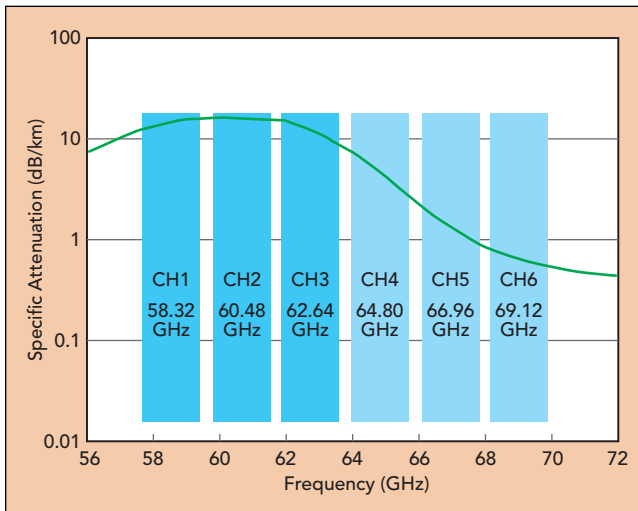
The range of the link corresponds to one or two city blocks, ideal for dense networks in urban areas where nodes are closely spaced in point-to-multipoint (PTMP) or mesh architectures. With careful channel allocation, these links can reuse the spectrum across an urban area without self-interference or causing interference to other networks. This capability enables a variety of use cases:

- Fixed wireless broadband, both backhaul and access.
- Outdoor Wi-Fi backhaul.
- Small cell backhaul.
- Video surveillance backhaul.
- Smart city IoT backhaul.

EXTENDING LINK DISTANCE

Previously, longer links could only be established using conventional point-to-point radio equipment with fixed, high gain antennas and the attendant high equipment, installation and alignment costs. Unfortunately, these conventional links are impractical for most fixed networks of any size and impossible for transportation networks. Alternatively, using spectrum with lower specific atmospheric attenuation enables longer-range PTMP and mesh networks using lower cost, more flexible phased array antenna systems.

In its "Spectrum Frontiers Report and Order," released on July 14, 2016 (FCC 16-89), the FCC opened the 64 to 71 GHz band for use by unlicensed devices, adopting the same technical standards set for the 57



▲ Fig. 4 Specific attenuation of the newer 64 to 71 GHz band, comparing 802.11ad channels 1 to 6.

to 64 GHz band, defined in section 15.255 of the FCC rules. The FCC noted the agency's action created a 14 GHz segment of contiguous spectrum to "encourage the development of new and innovative unlicensed applications and promote next-generation, high speed wireless links with higher connectivity and throughput, while alleviating spectrum congestion from carrier networks by enabling mobile data off-loading through Wi-Fi and other unlicensed connections."

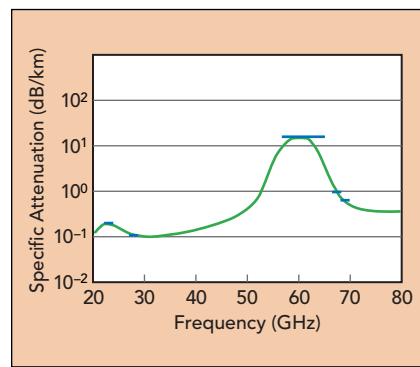
Ofcom, the U.K. regulator, conducted a "Fixed Wireless Spectrum Strategy" consultation in early 2018, resulting in a decision in July 2018 making the 64 to 66 GHz band unlicensed (it was previously coordinated by Ofcom) and opening the 66 to 71 GHz band for unlicensed use for 5G-like fixed wireless and mobile use cases. The Ofcom decision makes the U.K.'s spectrum allocation aligned with the U.S. allocation. The Ofcom decision and submissions from other parties are currently being reviewed by CEPT ECC, with the possible adoption of the same spectrum allocations more broadly through revisions to the ECC recommendations.

Using the same 802.11ad channel configuration, **Figure 4** shows the atmospheric attenuation for the newly

TABLE 2

LINK DISTANCE FOR A 16 Tx, 16 Rx TRANSCEIVER ON IEEE CHANNELS 2 AND 6

		Modulation and Coding		
	Units	MCS 8 QPSK	MCS 12 16-QAM	MCS 12.3 64-QAM
Maximum Average EIRP	dBm	40	40	37
Nominal Sensitivity	dBm	-89	-82	-77
System Gain	dB	129	122	114
Distance (Ch 2)	m	400	260	135
Distance (Ch 2), No Rain	m	460	290	150
Distance (Ch 6)	m	600	330	150
Distance (Ch 6), No Rain	m	> 700	420	170



▲ Fig. 4 Specific attenuation of the 24 and 28 GHz 5G bands vs. the extended 60 GHz band.

unlicensed spectrum and compared to channels 1 through 3. The attenuation in channels 4 through 6 is substantially lower than in the original unlicensed band, with the attenuation in channel 6 approaching 0.6 dB/km. Using the same system parameters described

above, significantly longer link distances can be achieved. **Table 2** compares the estimated link distances between channels 2 and 6, showing from a 50 percent increase for QPSK modulation to 11 percent for 64-QAM. The ability to support longer link distances of 300 to 400 m using channel 6 enhances the performance of existing applications and opens up new use cases:

- Use in suburban and lower density urban areas.
- Lower density small cell deployments.
- Long-range video surveillance.
- Wide area smart city IoT deployments.
- Transportation (e.g., trackside to train, roadside to bus, V2X).

A network operator can now deploy a less dense network in the upper part of the unlicensed band, increasing density over time by adding new links at lower frequencies. This potential can significantly improve the economics of a fixed network, and transportation applications, which require support for mobility over relatively long distances, become practical.

Interestingly, the specific attenuation in channels 5 and 6 of the newly allocated spectrum is comparable to that of the 5G licensed bands at 26 and 28 GHz (see **Figure 5**). While higher output power is permitted in the licensed bands, overall system performance is limited by the narrower channels and the higher order modulation required. The 66 to 71 GHz unlicensed band may be an equivalent alternative to the licensed bands for fixed wireless applications.

CONCLUSION

The availability of wide channels in the unlicensed 57 to 64 GHz band with the development of products using phased array antenna technology has made the development of dense, high capacity urban networks using novel mesh architectures practical. The addition of 64 to 71 GHz to the unlicensed band, with its lower atmospheric attenuation, enhances the scope of existing applications and offers new possibilities, especially in the transportation sector. Silicon process nodes with mmWave performance enable companies such as the Sivers IMA to develop transceivers covering the full 57 to 71 GHz band. This capability allows network operators and other service providers to exploit the potential of the unlicensed band.

Sidebar: Highly Integrated Silicon RFICs Enabling 57 to 71 GHz Phased Arrays

To use the abundant mmWave spectrum being allocated by regulators, operators must field compact and affordable base stations. Phased array architectures offer the best performance and flexibility for many use cases, yet the number of elements in the array, with transceivers at each element, demands seemingly conflicting transceiver requirements for high integration and low cost. Fortunately, the extension of silicon's economies of scale to mmWave frequencies over the last decade has created the technology platform enabling the development of these RFICs by companies such as Sivers IMA.

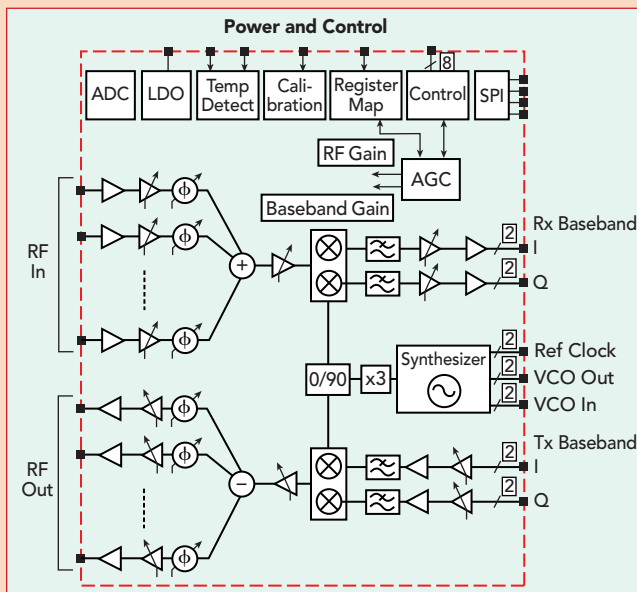
Sivers IMA's TRX BF01 is a highly integrated phased array RF transceiver developed for dynamic wireless communications infrastructure, such as mesh networks. It operates across 57 to 71 GHz and meets the IEEE 802.11ad specification, supporting channels 1 through 6, with center frequencies from 58.32 to 69.12 GHz. The transceiver integrates 16 Tx and 16 Rx signal paths and can be tiled into larger arrays (see **SB Figure 1**). The transceiver uses a direct conversion architecture for both Tx and Rx, connecting from the baseband modem to 60 GHz patch antennas via a low loss stripline connection.

The transmit path includes integrated linear power amplifiers, providing a combined output power of greater than 22 dBm. The receive path includes low noise amplifiers with 7 dB noise figure, providing excellent receiver sensitivity, and analog channel filtering to suppress out-of-band interference, making the transceiver robust

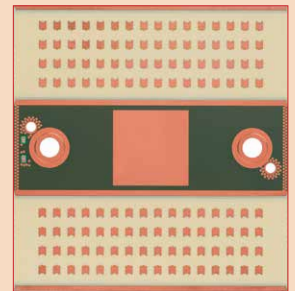
in a noisy RF environment and tolerant of out-of-band interferers. The transceiver includes a fully autonomous AGC, optimizing the receive gain based on the wanted and out-of-band signal levels, and provides autonomous DC offset and support for LO leakage and I/Q calibration. The error vector magnitude of -27 dB in both the transmit and receive modes supports modulation up to 64-QAM. High resolution phase shifters and signal path amplitude control enable accurate beamforming and reduced side lobes. The transceiver also contains a low noise VCO and fixed-N synthesizer and includes an auxiliary analog-to-digital converter to support various external functions, such as power and temperature measurements. With this level of integration, a complete transceiver system requires very few external components.

To address a range of use cases, the transceiver may be paired with various antenna array configurations. One common use is a distribution link for wireless mesh networks, which requires a link distance of several hundred meters combined with wide azimuth steering to address the different nodes in the mesh. In this scenario, the typical antenna design provides a horizontal steering range of 90 degrees with a fixed vertical beam. The corresponding half power beamwidth is 90 degrees horizontally, 20 degrees vertically. The antenna array can be implemented using a low loss laminate material, such as Megtron 6 or Rogers 3003, and standard printed circuit board fabrication. These materials are robust and proven and are cost-effective for high volume mmWave applications, such as wireless communications and automotive radar. Each antenna element has a gain of 10 dBi with flat frequency response from channels 1 through 6. The combination of the patch elements in a typical antenna array configuration with a single RF transceiver produces 16 Tx and 16 Rx antenna elements, providing 22 dB minimum gain on boresight (see **SB Figure 2**).

Combining the RF antenna module with a suitable baseband device, such as IDT's Rapidwave™ RWM6050, provides a complete 60 GHz communications subsystem, which is integrated with a network processor to create a wireless mesh network node. **SB Table 1** provides a system gain analysis, illustrating how the twin goals of wide steering range and long distance can be accomplished for a wireless mesh distribution network.



▲ SB Fig. 1 TRX BF01 transceiver block diagram.



▲ SB Fig. 2 The BFM06010 module integrates the transceiver RFIC and antenna array into 16 Rx and 16 Tx beamforming channels.

SB TABLE 1

BEAMFORMING MODULE PERFORMANCE IN CHANNEL 6 (69.12 GHz)

	Units	Modulation and Coding			
		MCS 4 BPSK	MCS 8 QPSK	MCS 12 16-QAM	MCS 12.3 64-QAM
PHY Rate	Mbps	1155	2310	4620	6757
Conducted Power	dBm	22.5	21	17	
Antenna Array Gain	dBi	23			
EIRP	dBm	45.5	44	40	37
Constrained EIRP	dBm	40	40	40	37
Element Sensitivity	dBm	-69	-66	-59	-54
Antenna Array Gain	dBi	23			
Receiver Sensitivity	dBm	-92	-89	-82	-77
System Gain	dB	132	129	122	114
Link Distance	m	750	600	330	150



Gapwaves Platform Integrates 5G mmWave Arrays

Carlo Bencivenni, Thomas Emanuelsson and Magnus Gustafsson
Gapwaves AB, Gothenburg, Sweden

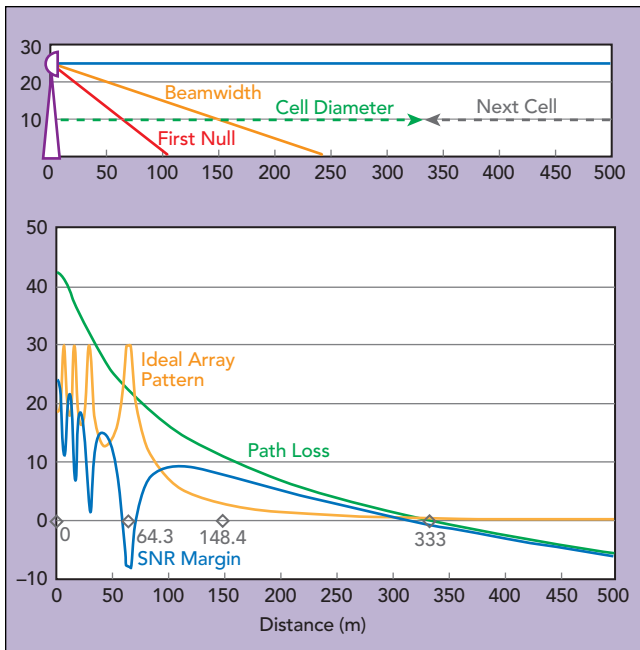
mmWave systems will have a key role supporting the massive data rates planned for 5G networks. However, unfavorable propagation and technical limitations challenge the feasibility and adoption of such systems. Addressing these challenges, Gapwaves is developing waveguide technology with superior performance over conventional printed circuit board (PCB) solutions, including exceptional efficiency, routing, subarray partitioning, filtering, isolation and thermal handling. With improvements in performance, range, number of components and power consumption, the hardware, deployment and operating costs can be significantly reduced. This article discusses the design principles and results of Gapwaves' demonstration platform, including both passive and active measurements, and the integration of high-power GaN semiconductors to further enable the vision of high performance and cost-effective mmWave systems.

5G, the next-generation mobile network, has a large set of ambitious objectives, leveraging multiple technologies for several different application scenarios.¹ Within those, the 100× increase in network capacity compared to the current 4G network will be the most visible to the consumer. Traditional sub-6 GHz frequencies will continue to be the backbone for ubiquitous connectivity, with a boost in capacity from additional bands and advances in coding. However, such a dramatic increase in data rates heavily depends on massive amount of spectrum: GHz of bandwidth available in the mmWave region at a lower cost per Hz. Regulatory bodies have identified several bands for this, mostly between 24 and 60 GHz.

Moving to the mmWave region raises technical issues. The coverage from a base station is considerably less than that of existing systems, due to large propagation losses and severe shadowing and penetration effects from obstructions by buildings, trees and people.

mmWave active components generate low output power with low efficiency, with smaller size creating problems with component and power density. This results in limited transmit power, high power consumption and expensive components. Typically, all components suffer from increased losses with frequency, which can become onerous for planar technologies at high frequencies. Also, satellite and backhaul services coexist in the mmWave region, requiring RF filters to prevent interference, which increases system losses.

Deployment of 5G mmWave systems will be driven by household fixed wireless access (FWA) first, with mobile access later. The success of the former depends on base station coverage; to strengthen the business case in suburban areas, higher inter-site distance (ISD) and equivalent isotropic radiated power (EIRP) are needed.² Higher EIRP increases capacity in systems with hybrid and digital beamforming, where the additional power can be shared across multiple beams and users.

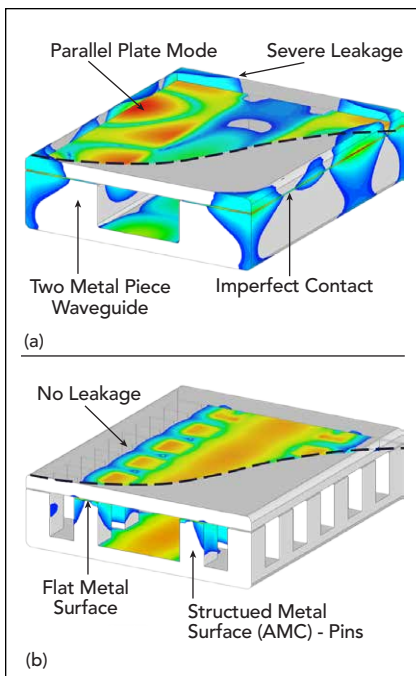


▲ Fig. 1 SNR margin relative to the cell edge for an 8-element vertical subarray with no downtilt and 333 m cell radius.

mmWAVE APPLICATIONS

The industry response to the above challenges has mainly been planning small cell, high capacity coverage. However, while a denser deployment will be unavoidable, the economic feasibility and widespread availability depends on the technical solutions and associated cost. The number of base stations per area determines the cost for equipment, deployment and operation.

Recently, the first demonstration products were released by major telecommunications equipment manufacturers.³ Most



▲ Fig. 2 Imperfect joints in standard waveguide cause leakage and spurious modes (a) compared to the fields in a Gapwaves waveguide (b).

of the current systems are based on integrated PCB antennas, typically with a patch array on the front of the board and active components on the back side. Losses are minimized by vertically routing through the PCB in a one-feed-per-antenna configuration, at the expense of low gain. As a result, achieving high EIRP and downlink coverage are challenging. To partially compensate, a large number of active chains are used, increas-

ing the cost of the system and the power consumption. However, the increased power at the base station, as opposed to the gain, does not help the uplink, which is the hardest leg. The tight integration and high power consumption in a very limited space of a multi-layered PCB create thermal handling and complexity issues. Another challenge is integrating filters and their impact on performance, which is substantial at these frequencies. All these limitations ultimately result in poorer performance, reduced range, higher power consumption and increased cost. The solution by some suppliers is to increase the system size, resulting in a large number of expensive components.

Taking a different approach, Gapwaves is focusing on maximizing antenna gain and minimizing feed and filtering losses, to increase system range and performance and increasing component output power. Most importantly, low loss subarrays can be used to increase gain, with the trade-off of reduced elevation coverage, as the beam narrows and grating lobes appear. In real scenarios, however, a user's angular distribution in elevation is extremely limited, especially for suburban FWA with low buildings. As shown in **Figure 1**, even an 8-element, vertical subarray with no downtilt or elevation scanning provides adequate signal level at all distances for a 500 m ISD (333 m cell radius), despite an elevation beamwidth of about 12 degrees. This is valid as long as no deep notches are present in the elevation pattern.

WAVEGUIDE REVISITED

The primary transmission technologies for microwave applications are metal waveguide and substrate-based PCBs. While the former offers unmatched performance, its bulkiness, cost and complexity have limited applications to niche, high-end markets such as satellite and military. PCBs offer planar, robust, cost-effective solutions with satisfactory performance and, for these reasons, have long been the standard for commercial solutions.

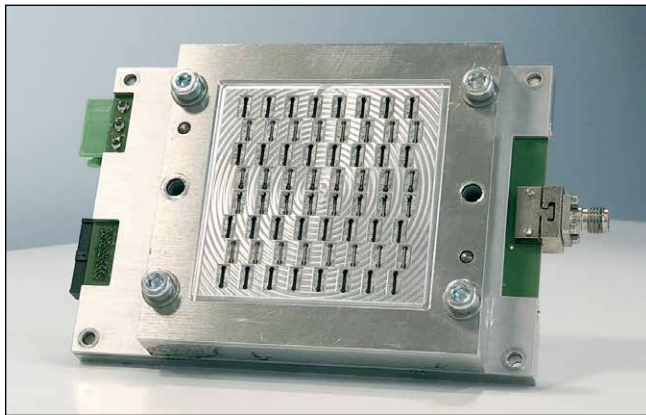
However, both technologies face severe challenges at mmWave frequencies. PCB losses are substantial: at 30 GHz, conventional PCB microstrip lines with high frequency substrates suffer losses in the 10s of dB/m, compared to fractions of dB/m for waveguide. PCB designers must compensate by using premium substrates and minimizing trace lengths; however, as frequencies increase, the losses become overwhelming. Waveguide suffers from increasingly impractical manufacturing tolerances as frequencies increase. A rectangular waveguide with a joining defect on the order of micrometers between its two parts suffers catastrophic leakage (see **Figure 2a**). Split-block design best practices and high quality joining processes improve performance but are not suitable for mass manufacturing.

A solution is offered by Gapwaves, a robust and low loss technology developed at Chalmers University of Technology by Professor Per-Simon Kildal and his research group.⁴ By using an artificial magnetic conductor surface, typically realized with a bed of pins, robust waveguide-like transmission lines and components can be created without needing electrical contact between the layers. As shown in **Figure 2b**, the equivalent Gap-

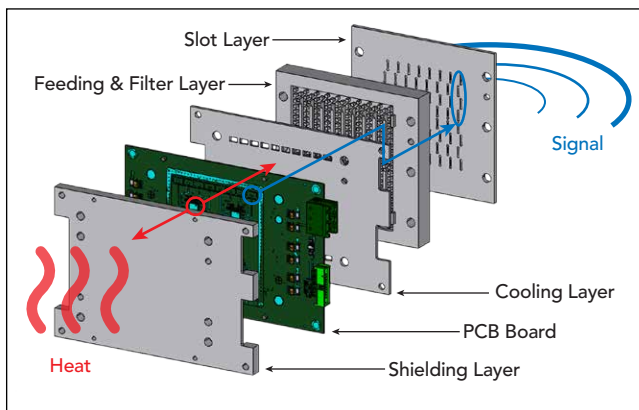
waves waveguide performs flawlessly with a gap present, containing the fields within a few rows of pin and with comparable losses. No joining process is necessary. This key aspect enables a waveguide to achieve both premium performance and cost-effective manufacturing for consumer markets. Gapwaves AB was founded in 2011 with the objective of developing and commercializing Gapwaves waveguide solutions.

GAPWAVES WAVEGUIDE 5G ANTENNA

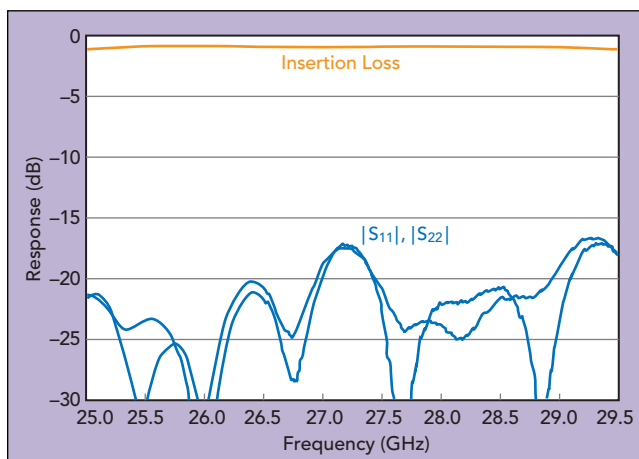
To demonstrate the advantages of Gapwaves waveguide, we have developed a demonstration platform including the key passive and active components, al-



▲ Fig. 3 Gapwaves 28 GHz demonstration array.



▲ Fig. 4 Exploded view of the Gapwaves waveguide array.



▲ Fig. 5 Back-to-back measurement of the transition through a four-layer FR4 board.

though the focus is on the antenna and RF performance (see **Figure 3**). Typical requirements have been considered; as a result, the design is not tailored for any specific application.

The center frequency is 28 GHz, in line with U.S. 5G trials, and the target bandwidth is greater than 13 percent to accommodate current 5G bands. A 1.2 GHz filter is integrated in each subarray feed to support analog, digital and hybrid beamforming and the typical instantaneous bandwidths. Full scanning is provided in azimuth and reduced in elevation. A spacing of $\lambda/2$, approximately 5.5 mm, and 4-element vertical subarrays were adopted to guarantee ± 45 and ± 10 degree scanning in azimuth and elevation, respectively. The demonstration antenna is an 8×8 array. Although a smaller size, it is sufficient to fully characterize the system and extrapolate to larger sizes without unnecessary complexity. Due to the subarrays, 16 feeds are present. SiGe front-ends are used, which provide a total EIRP of 44 dBm based on typical SiGe RFIC performance.

As shown in **Figure 4**, the system is a multi-layer, largely metal assembly. The PCB, with the active components, is located between the shielding layer on the back and the cooling layer on the front. The shielding layer improves isolation and cavity mode suppression, and the cooling layer hosts the transitions to the antenna. Both layers are key to thermal performance. From the PCB, the RF is routed to the filter and distribution layer, which provides low loss routing, the subarray feeds and dedicated filters. Finally, the slot antenna is the front layer.

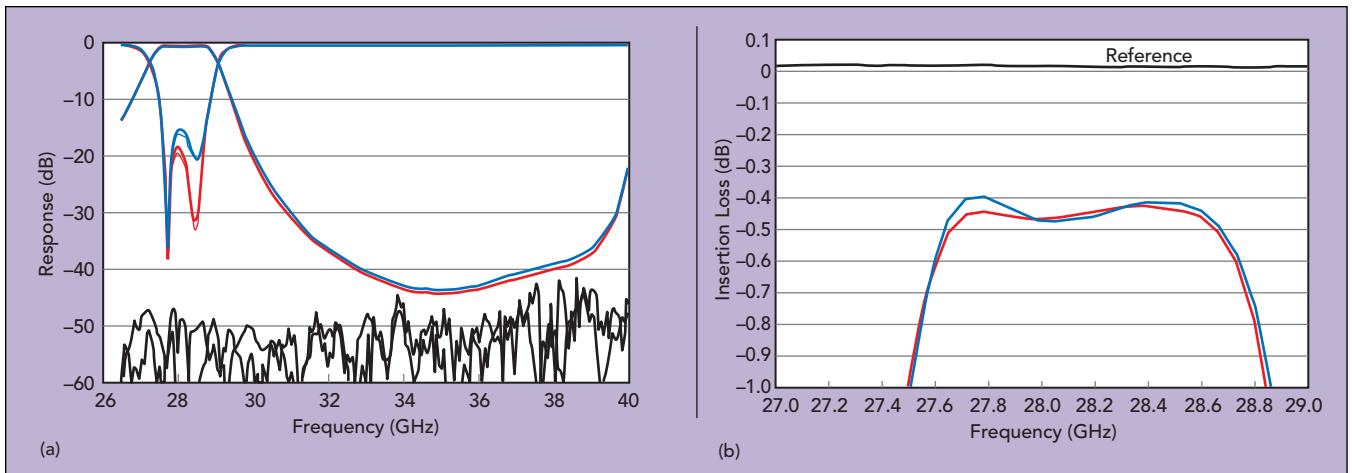
Transitions

One of the key advantages of Gapwaves waveguide technology is the low loss nature of its interconnections, typically more than $10 \times$ better than equivalent PCB solutions. It is highly desirable to transition from the PCB hosting the digital and low frequency signals to waveguide as soon as the RF signal is generated, performing high frequency functions such as filtering and routing in waveguide. The transition between PCB and waveguide should guarantee a low loss, robust and contact-less interface.

While a variety of transitions have been designed and manufactured, a through-substrate configuration has been adopted. This allows positioning the components facing backward in direct contact with the heat-sink. Since the signal travels from the microstrip vertically through the substrate, different transition versions have been designed depending on the PCB stack-up. A single transition with a two-layer 10 mil Rogers RO4350 board has a measured insertion loss of 0.2 dB and return loss of 20 dB over a 20 percent bandwidth. **Figure 5** shows a back-to-back measurement of a four-layer board with a 10 cm waveguide line section. Tolerance analysis and repeated measurements prove the robustness of the design to assembly variations.

Filtering

RF filters are needed to protect sensitive services, such as the passive Earth Exploration Satellite Service (EESS).⁵ The EESS band extends to 24 GHz, and the low end of the 5G n258 band starts at 24.25 GHz—only 1



▲ Fig. 6 Measured performance of two 28 GHz Gapwaves waveguide bandpass filters showing wideband performance (a) and passband insertion loss (b).

percent frequency margin. Meeting emission limits requires sharp filter rejection or an expensive guardband. While several filter technologies could be applied, they can introduce considerable loss, use scarce PCB area and cause complicated routing.

Gapwaves waveguide technology enables waveguide filters integrated in the antenna, offering premium performance and eliminating complexity. While waveguide filters are well known and used in high performance applications, the amount and density of the filters pose the main challenges for the gap waveguide design. Achieving the filter area, constrained by the antenna element spacing to approximately $0.5\lambda \times 2\lambda$, is extremely challenging, as the area includes the division walls or pins between the subarrays and transitions between layers. Since the array will contain tens to hundreds of filters which must be functional as assembled without tuning, the design must be extremely robust to manufacturing and assembly. While the pin structure of the Gapwaves waveguide helps with the robustness, the design of the filter resonator is crucial. The design for meeting these requirements is less than about $\lambda/2$ in x, y and z.

For the demonstrator antenna array, the filter design is a third-order Chebyshev with 1.2 GHz bandwidth (20 dB return loss) centered at 28 GHz. The measured performance of two filters is shown in **Figure 6**. The insertion loss is 0.4 dB, compared to an equivalent microstrip filter which would have losses of several dB. Although the filter fits comfortably under each subarray, for these measurements it was positioned on the auxiliary through line to characterize the filter independent of the antenna.

Antenna

The demonstrator antenna is an 8×8 slot array organized as 4-slot subarrays in an eight column, two row configuration (see **Figure 7**). As the subarray is periodic, the antenna can be extended in both horizontal and vertical directions. The $\lambda/2$ spacing and vertical grouping enable scanning without grating lobes beyond 45 degrees in azimuth and up to 10 degrees in elevation. The demonstrator antenna has a single polarization. Both vertical and horizontal versions of the antenna have been developed and tested, although this article only

presents results from the single polarization antenna.

The subarray is a series, end-fed resonant slotted waveguide. The antenna covers the band from approximately 26.5 to 31 GHz, greater than 15 percent relative bandwidth. The measured and simulated array patterns show very good agreement (see **Figure 8**), with no notches



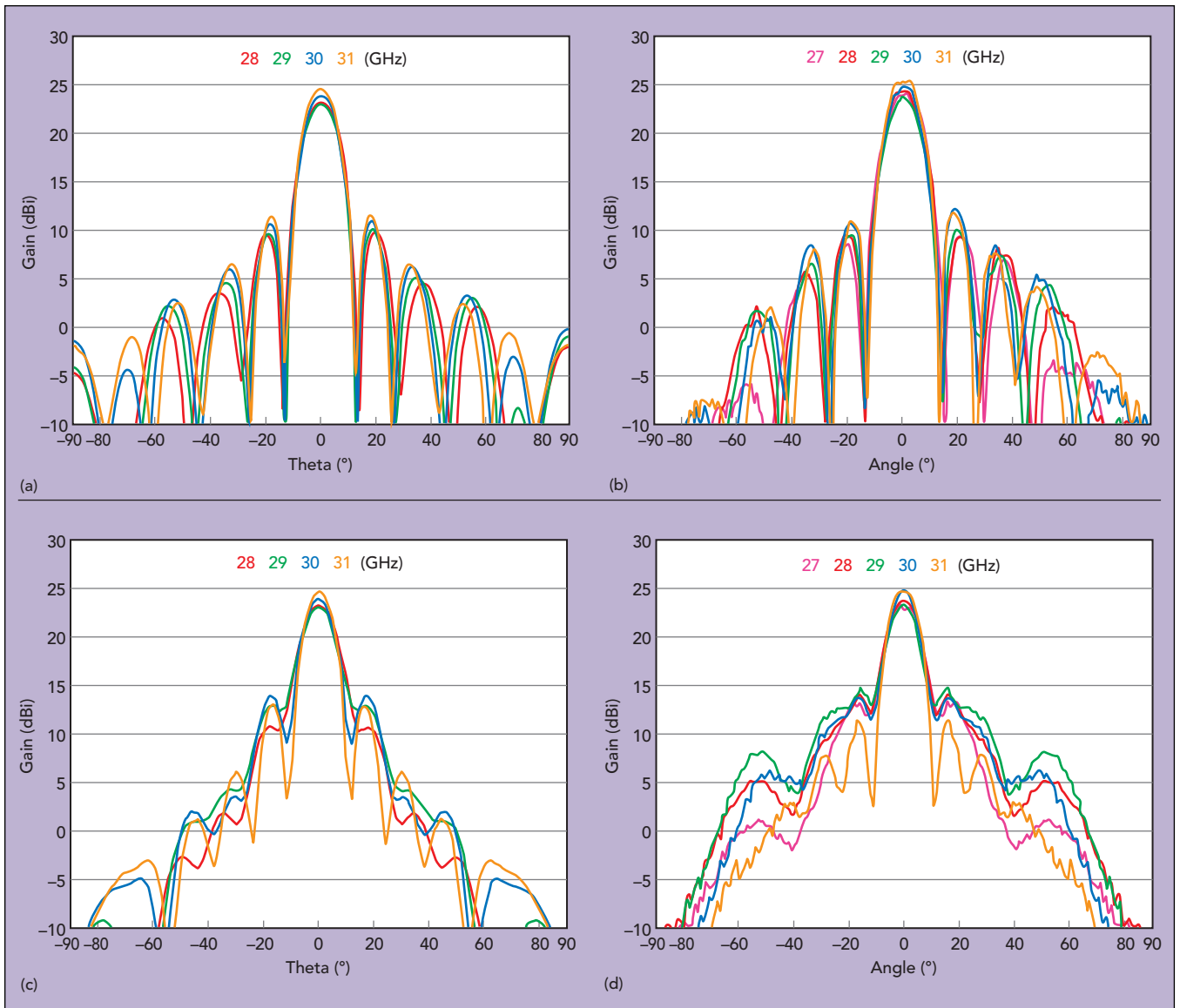
▲ Fig. 7 The single polarization Gapwaves antenna is an 8×8 slot array configured as 4-slot subarrays in eight columns and two rows.

in the elevation patterns. The antenna has a total gain of 24 dBi, 12 dBi per subarray per channel. Embedded matching is better than 20 dB, isolation better than 16 dB and active matching better than 10 dB over all scan angles.

Thermal Design

Thermal handling is challenging at mmWave frequencies, where the many densely packed components create substantial heat in a limited area. High thermal handling is critical to ensure semiconductor and other components operate within their specified operating temperature ranges, assuring reliability and optimum performance. A SiGe IC solution for a mmWave, dual polarized array, for example, dissipates several W/cm^2 . The thermal situation is complicated by the desire for passive cooling, which is challenging for a system dissipating more than a few hundred Watts. For even moderate heat dissipation, PCB designs rely on using thermal vias.

A Gapwaves waveguide system has excellent thermal capabilities. The all-metal antenna assembly doubles as an integrated heatsink, extracting heat from both the top and bottom sides of the components. Back-of-the-



▲ Fig. 8 Gapwaves array antenna patterns: azimuth simulated (a) and measured (b), elevation simulated (c) and measured (d).

envelope calculations show that the antenna assembly can extract up to 2 W/°C from top-sided cooling of a typical 5 mm × 5 mm component area. The subarray architecture also provides benefits: for a fixed EIRP, it reduces the required power and decreases component density.

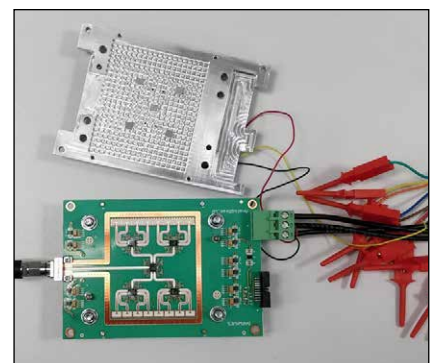
Measurements of the demonstration platform confirmed the effectiveness of the design using top-side cooling of the SiGe ICs. The steady state temperature measured by the on-chip sensors at maximum output power was only 60°C, when maximum junction temperatures are typically around 150°C.

ARRAY PERFORMANCE

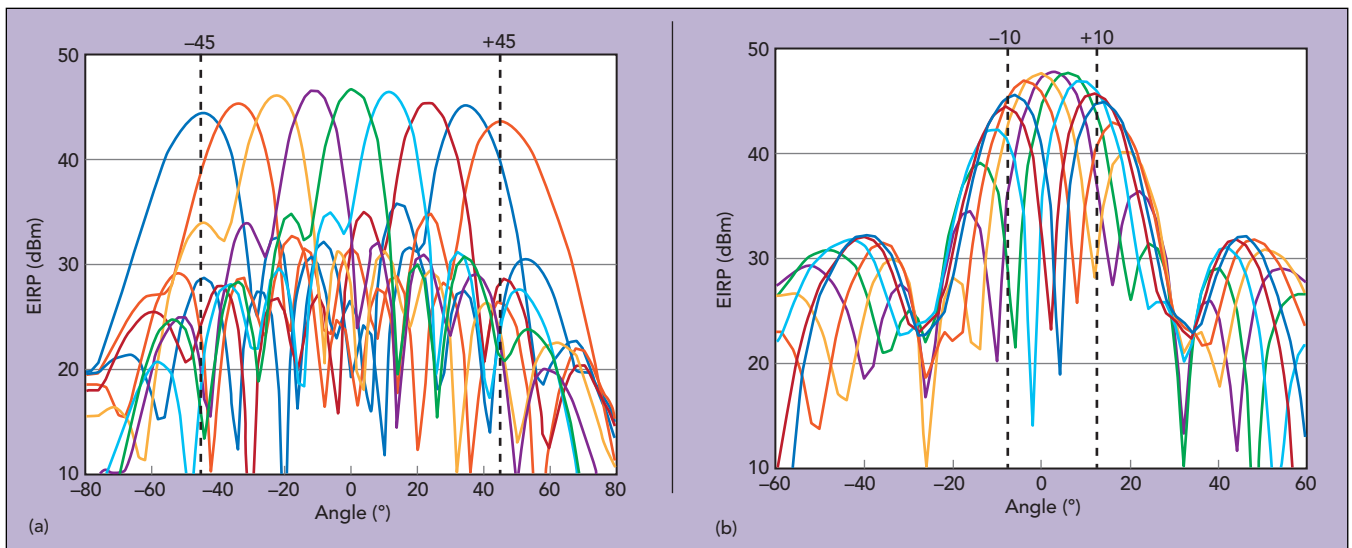
The active part of the demonstration platform consists of an analog beamforming board using commercially available components (see **Figure 9**). The 16 antenna ports are fed by four SiGe ICs, each with four Tx/Rx channels and connected to a single input/output RF connector. A fifth IC on the board serves as an optional

buffer and preamplifier. The SiGe Tx/Rx chains provide 17 dBm saturated output power per channel, backed off to 8 dBm per channel to ensure good linearity. The amplitude and phase of each port can be independently controlled digitally, enabling full control of the beam. The total power consumption is about 13 W. The ICs operate from 26.5 to 29.5 GHz, less than the bandwidth of the antenna.

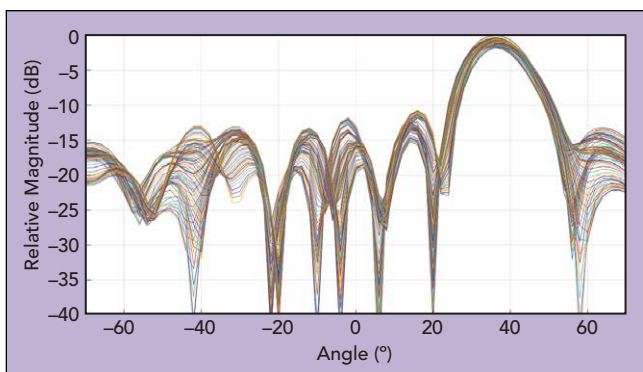
Active measurements validate the system performance in both Tx and Rx. Only the Tx results are pre-



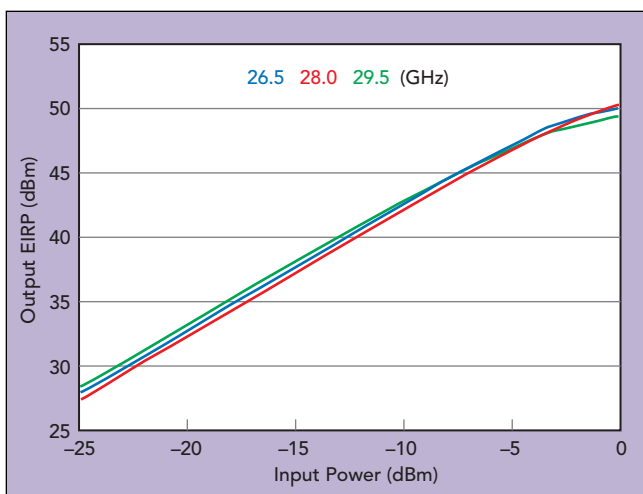
▲ Fig. 9 Analog beamformer board.



▲ Fig. 10 Gapwaves array azimuth (a) and elevation (b) beam steering using analog beamforming.



▲ Fig. 11 Azimuth antenna pattern vs. frequency, 26.5 to 29.5 GHz, no calibration.



▲ Fig. 12 Measured antenna EIRP.

sented here, with the measured antenna beams shown in **Figure 10**. The beams are well behaved: scanning beyond the design requirements of ± 45 degrees in azimuth and ± 10 degrees in elevation and stable over frequency (see **Figure 11**). The measured EIRP is approximately 52 dBm at saturation, backed off to 44 dBm with an error vector magnitude (EVM) of approximately 3 percent (see **Figure 12**).

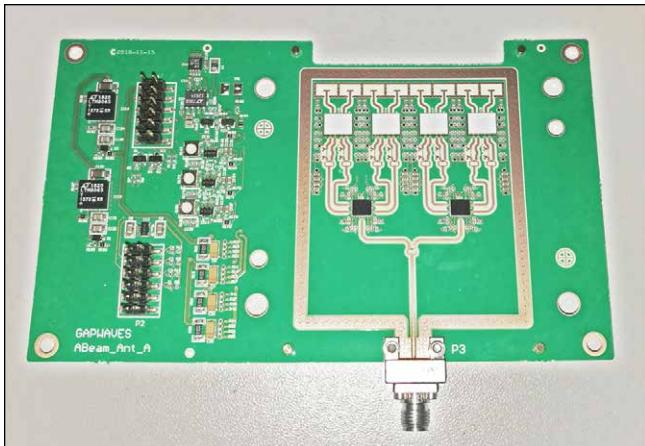
INCREASING EIRP

To increase the EIRP of mmWave arrays, a logical step is to adopt GaN on SiC in the RF front-end. Originally developed for defense applications, GaN technology has matured and the cost is becoming competitive for commercial applications.² Its high breakdown, electron mobility, power density and excellent thermal properties make the compound semiconductor attractive for mmWave front-ends. For Tx, GaN achieves a saturated power of 2 W with a power-added efficiency of approximately 10 percent. Backed off to an EVM of 3 percent, GaN can deliver an average output power of 24 dBm. GaN also achieves a noise figure about 1.5 dB better than SiGe, which significantly improves the uplink margin.

However, the high-power density of GaN requires considerable cooling capability in the antenna array, even though GaN's maximum rated junction temperature is about 75 degrees higher than SiGe. The Gapwaves waveguide approach offers the thermal handling needed for GaN power amplifiers. Although Gapwaves is agnostic to the choice of semiconductor technology, combining the low loss, high gain waveguide array with the high-power and high efficiency of GaN is very attractive. The combination can reduce the number of components and power consumption for a given EIRP, reducing the cost of the array. A gap waveguide antenna using a GaN front-end is being developed for the 28 GHz band (see **Figure 13**). The subarray design contains eight slots in a single row, using analog beamforming with a GaN front-end module. Eight subarrays can be combined to form a 64-slot antenna with 24 dBi gain and 56 dBm EIRP at 9 dB back-off. The array will scan ± 45 degrees in azimuth, and no elevation scan is planned. A total power consumption of about 40 W is expected.

SUMMARY

Gapwaves' demonstration platform shows the performance capabilities of the Gapwaves waveguide technology for mmWave antenna arrays. The low loss



▲ Fig. 13 Analog beamformer using GaN front-end modules.

and thermal advantages of waveguide; the ability to integrate antennas, filters, radio and baseband components; and a cost-effective, producible platform position this technology as a strong contender for 5G and other mmWave systems. While the platform is agnostic to RF semiconductor technology, its thermal performance is particularly beneficial for the high-power density of GaN.■

References

1. International Telecommunications Union, ITU-R Radiocommunications Sector of ITU, "IMT Vision—Framework and Overall Objectives of the Future Development of IMT for 2020 and Beyond," August 2015.
2. B. Peterson and D. Schnauffer, "5G Fixed Wireless Access Array and RF Front-End Trade-Offs," *Microwave Journal*, Vol. 61, No. 2, February 2018, pp. 22–43.
3. Ericsson, "AIR 5121 Pre-NR Base Radio in FCC ID TA-8AKRD901059-1," fccid.io/TA8AKRD901059-1.
4. P. S. Kildal, E. Alfonso, A. Valero-Nogueira and E. Rajo-Iglesias, "Local Metamaterial-Based Waveguides in Gaps Between Parallel Metal Plates," *IEEE Antennas and Wireless Propagation Letters*, Vol. 8, 2009.
5. 3GPP Technical Specification Group Radio Access Network, "Study on New Radio Access Technology: RF and Co-Existence Aspects," TR 38.803 V14.2.0, <https://portal.3gpp.org/desktopmodules/Specifications/SpecificationDetails.aspx?specificationId=3069>.



Optimize 5G SNR with beamforming partitioning between the RF and digital domains

Use MATLAB® and Simulink® to

- Design MIMO phased arrays
- Partition hybrid beamforming across RF and baseband domains
- Model MIMO wireless communication systems
- Explore architectural choices and tradeoffs
- Evaluate the quality of the partitioning design

Read the white paper:

Exploring Hybrid Beamforming Architectures for 5G Systems

Multi-Beam Phased Array with Full Digital Beamforming for SATCOM and 5G

Divaydeep Sikri and Rajanik Mark Jayasuriya
SatixFy UK Ltd., Farnborough, U.K.

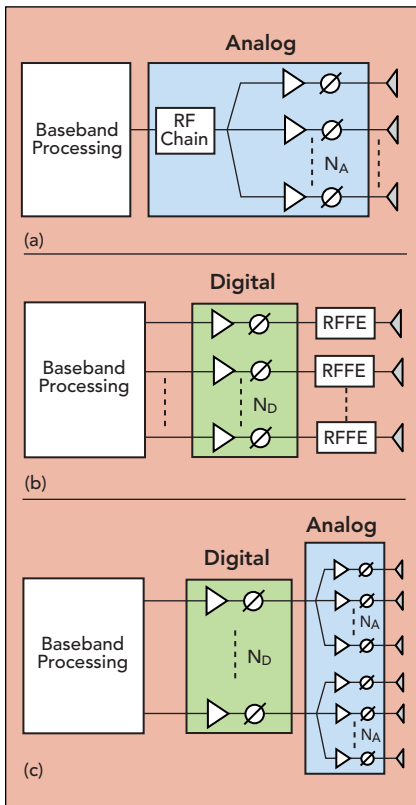
As we usher in the age of large capacity wireless access systems demanding high spectral efficiencies, array antennas are playing an increasing role. MIMO antenna arrays have become integral to the standards for cellular and wireless local area networks. These active antenna arrays will play an equally important role in next-generation high throughput satellite (HTS) communications. Also, the large low Earth orbit (LEO) and medium Earth orbit (MEO) constellations planned by companies like OneWeb, Telesat, SES and SpaceX will need ground terminal antennas that track multiple satellites. This convergence of trends is driving a shift from passive antennas with static fixed beam patterns to fully steerable, active smart antennas. In this article, we discuss the advantages of digital beamforming (DBF) for capacity, control and flexibility. Until now, DBF was largely a concept because of the cost and complexity to implement a usable solution. We will describe a commercial ASIC implementing DBF with true time delay (TTD) that realizes its potential. DBF combined with an integrated RF front-end (RFFE) enables modular electronically-steerable multi-beam array (ESMA) antenna systems for a wide range of applications.

Mobile wireless communications systems require increasingly high data rates with virtually worldwide coverage. Because terrestrial networks do not cover the globe, high data rate services are not available in remote areas or onboard ships and aircraft. SATCOM and SATCOM-on-the-move (SOTM) are essential capabilities to achieve high capacity communications with global coverage. With large capacity wireless access requiring high spectral efficiency, array antennas have emerged as a key architecture for wireless communication systems, and MIMO antenna arrays are included in the standards for cellular and wireless local area networks. These ac-

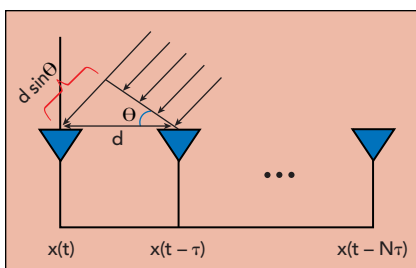
tive antenna arrays will play an equally important role in next-generation HTS communications. The development of large LEO and MEO constellations, planned by companies like OneWeb, SES and SpaceX, will require ground terminals able to track multiple satellites. Parabolic dish antennas have been the defacto design for SATCOM Earth antennas. They have advantages such as good performance, power consumption and cost, yet they are stationary and have lower efficiency. In comparison, electronically-steerable antennas have many benefits: self-installation, multi-SATCOM, satellite tracking and their payloads can be more flexible, enabling techniques such as multi-beam, beam hopping and

flexible beam shaping. All-electronic control eliminates mechanical parts, which are slow and more likely to malfunction.

As Ku-Band capacity is widely available from the existing geostationary (GEO) satellite networks above the planet, market interest has largely been for satellite services at Ku-Band, namely digital TV broadcast, broadband internet access and IoT networks. The growth of these services will depend on the development of new high performance and low-cost user terminals with the ability to track satellite position while in motion. The antenna at the terminal must be capable of wide-angle scanning while keeping fabrication costs as low as possible, since most applications are consumer markets. For low-cost applications such as the IoT, the cost of the antenna can be reduced using energy efficient waveforms, such as half-duplex, which optimize link and resource utilization. The cost using such waveforms can be reduced with a single antenna that can serve both receive (Rx) and transmit (Tx).



▲ Fig. 1 Analog RF (a), digital (b) and hybrid (c) beamformers.



▲ Fig. 2 Uniform linear array geometry.

BEAMFORMING OPTIONS

Antennas convert RF signals into electromagnetic transmission and vice versa. Each antenna has a radiation pattern defining the direction of the energy radiated by the antenna. An antenna's gain and directivity go hand in hand: the greater the gain, the more directive the antenna. It is this feature of the antenna that has become the focus for increasing capacity, particularly with the next-generation of wireless communications systems for both SATCOM and 5G.

Beamformers comprise an array of antennas making the combined aperture directive. They control the radiation pattern through the constructive and destructive superposition of signals from the

different antenna elements. In general, beamforming can be classified as passive and active. Passive beamformers are fixed directive antennas made of passive components, such as transmission lines, that point the beam in a fixed direction. Active beamformer antennas—commonly known as phased arrays—have active phase shifters at each antenna element to change the relative phase among the elements; because they are active, the beam can be dynamically steered. Electronically-steerable antennas can adopt one of three approaches to beamforming: analog, digital and hybrid (see **Figure 1**).

Analog Beamforming

Analog beamforming (ABF) can be implemented in three ways: RF, local oscillator (LO) and analog baseband.

With RF beamforming, phase shifting is implemented in both the RF Rx and Tx paths prior to the mixer. Reduced component cost is one of the reasons for its popularity, particularly at mmWave, where the small size of the phase shifter allows better integration in the RFFE. However, phase shifter precision and noise figure degradation due to the phase shifters are performance challenges for this technique. Also, the phase shifters and beamforming network (BFN) must be designed for the frequency of operation.

LO beamforming uses the LO distribution network for phase shifting, addressing the noise figure challenge by shifting the phase shifter from the signal path to the LO path. However, this increases power consumption, and the complexity scales with the size of the antenna.

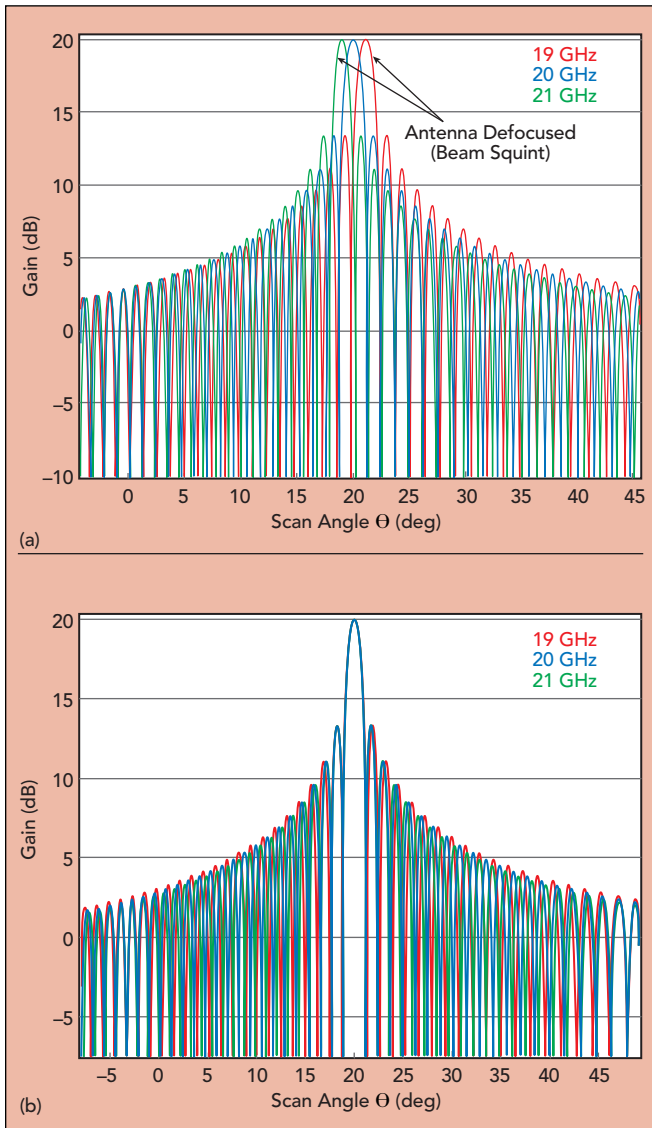
With analog baseband beamforming, beamforming occurs in the baseband, after down-conversion and before up-conversion, enabling use of higher precision phase shifters. However, the size of the phase shifters and the complexity of the BFN—mixers in each RF chain and a network of baseband splitters and combiners—are challenges.

Digital Beamforming

With digital beamforming (DBF), beamforming is performed digitally at baseband, requiring one beamformer and RFFE at each antenna element. Offering a high degree of control, DBF is considered the most flexible beamforming approach and superior to ABF for receiving and transmitting wideband signals and, more importantly, for multi-beam applications. The digital implementation has greater reconfigurability and enables treatment of RF impairments at each antenna element. However, it requires data converters and RFFEs for each antenna element, increasing the complexity and power consumption. Fortunately, recent advances in silicon processes have reduced the complexity, power and cost of digital beamforming, making it feasible for some phased arrays.

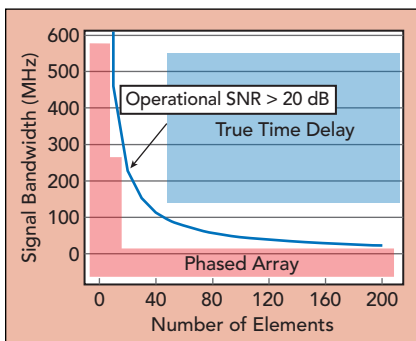
Hybrid Beamforming

Hybrid beamforming uses the best of both alternatives: analog and digital. To reduce the complexity of digital beamforming, requiring control at each antenna element, the hybrid approach uses "two stage"



▲ Fig. 3 Phased array radiation patterns showing beam squint vs. frequency (a) and no beam squint with true time delay (b).

beamforming—the concatenation of analog and digital beamforming—and provides a reasonable compromise between performance and complexity. Each analog beamforming network serves as a subarray for the next level of digital beamforming, forming a more directive “super element” whose signal is coherently combined in the digital domain with the signals from the other super elements. Hybrid beamformers provide limited multi-beam capability, although the performance is sub-optimal compared to digital beamforming.



▲ Fig. 4 Maximum signal bandwidth vs. number of elements in a uniform linear array.

DIGITAL BEAMFORMING WINS

Given the ongoing improvement in silicon technology, DBF is the preferred approach for phased array antennas. It offers:

Wideband signal reception and transmission: Wider signal bandwidth improves the spectral efficiency of the system, increasing the capacity of the terminal. DBF enables ready implementation of high precision phase shifters and delay compensation (TTD), so the array can operate over a large signal bandwidth without beam squint.

Ability to scale to build large antennas: To build large antennas, the beamformer architecture should be modular to enable relatively simple scaling. To reduce beam squint, large antennas need to correct for the delays from scanning and system routing, which becomes more challenging with large antennas. DBF supports modular design and can easily scale while maintaining performance.

Large number of beams: MIMO with multi-beam capability is the most effective way to increase channel capacity. With SATCOM, it enables simultaneous communication with multiple satellites. DBF supports large numbers of beams using the entire antenna aperture, which provides the same antenna gain and directivity for each beam.

Fast beam steering: DBF supports fast beam switching and steering, i.e., within microseconds. This enables fast acquisition and tracking in high dynamic channel environments.

Flexibility: Active beamforming with flexible reconfiguration enables the array to adapt for multiple applications, such as online calibration, configuring dynamic subarrays and monitoring processing and synchronization.

Precise beamforming and nulling: With precise control of the phase and gain, DBF enables fine control of the radiation pattern, including side lobes, null depth and null positioning. This fine control can form the radiation pattern to meet regulatory masks and suppress unwanted directional interference, maintaining a high signal-to-noise ratio (SNR).

Antennas on conformal structures: The ability of DBF to calibrate and compensate for phase and delay allows decoupling the antenna’s geometry from its performance, making conformal antennas feasible, i.e., unrestricted to a 2D plane. Geometric shapes such as hemi-spheroidal 3D antennas or other conformal shapes can be implemented using DBF.

TTD BEAMFORMING

As shown in **Figure 2**, with a uniform linear array, the incident wavefront at an angle θ results in a delay ($\tau \dots N\tau$) for the signals arriving at different elements. This delay causes the antenna array to have a pattern depending on the frequency. To have a flat pattern over the desired frequency range, the antenna’s coherent bandwidth should be greater than the bandwidth of the signal. This implies that $N\tau \ll T_s$, where T_s is the duration of the symbol. This condition requires the system to have the capability to perform delay compensation to coherently



▲ Fig. 5 SatixFy Prime DBF ASIC.

relative to symbol duration if either the antenna is very large (N) or the symbol duration is very small (T_s), i.e., the bandwidth is very large. This point is illustrated in **Figure 4**.

SatixFy has developed the industry's first TTD DBF in a form that is efficient in power and cost (see **Figure 5**). The Prime ASIC has a modular and flexible architecture supporting real-time reconfiguration, online calibration and the scalability to build large antennas. Prime digitizes the signal at each antenna element with high speed analog-to-digital converters (ADC) and digital-to-analog converters (DAC), processing more than 2 Tbps data rates. Prime connects to RFFE's containing the RF transceivers via a high bandwidth I/Q interface. Within each DBF, the ADCs and DACs are connected to high-resolution digital phase shifters and digital delay circuits

combine signals. **Figure 3** shows the beam squint resulting from the frequency selectivity of an array, which does not occur with TTD beamforming.

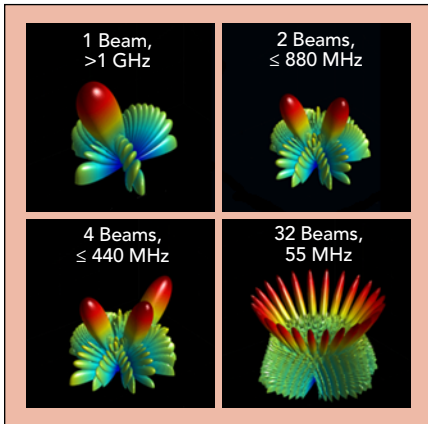
The relationship $N\tau \ll T_s$ indicates the antenna's delay spread can become very large

which implement TTD to avoid beam squints, enabling wideband signal transmission and reception. The DBF chips are connected to each other via a high speed digital serial bus (SERDES), which enables a highly integrated, controllable and scalable antenna system. The key features of the Prime DBF are:

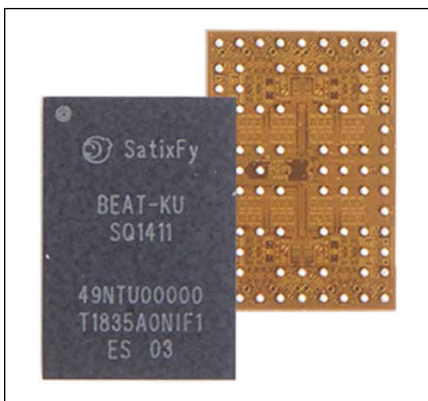
- Over 1 GHz instantaneous signal bandwidth.
- Multi-beam capability: up to 32 beams with independent phase, gain and delay control for each beam (see **Figure 6**).
- Equalization/pre-equalization and digital predistortion for each beamformer chain.
- 2 GHz analog baseband interface.
- Tight integration with SatixFy's Sx3000 modem via SERDES interface.
- Support for an external modem with an L-Band interface.
- Very high speed beam tracking and beam steering.
- Linear and circular polarization control.
- Self-calibration with internal synchronization engines.
- Antenna control integrated with the Sx3000 modem.
- Power saving modes and configurations tailored to the application.

RF TRANSCEIVER

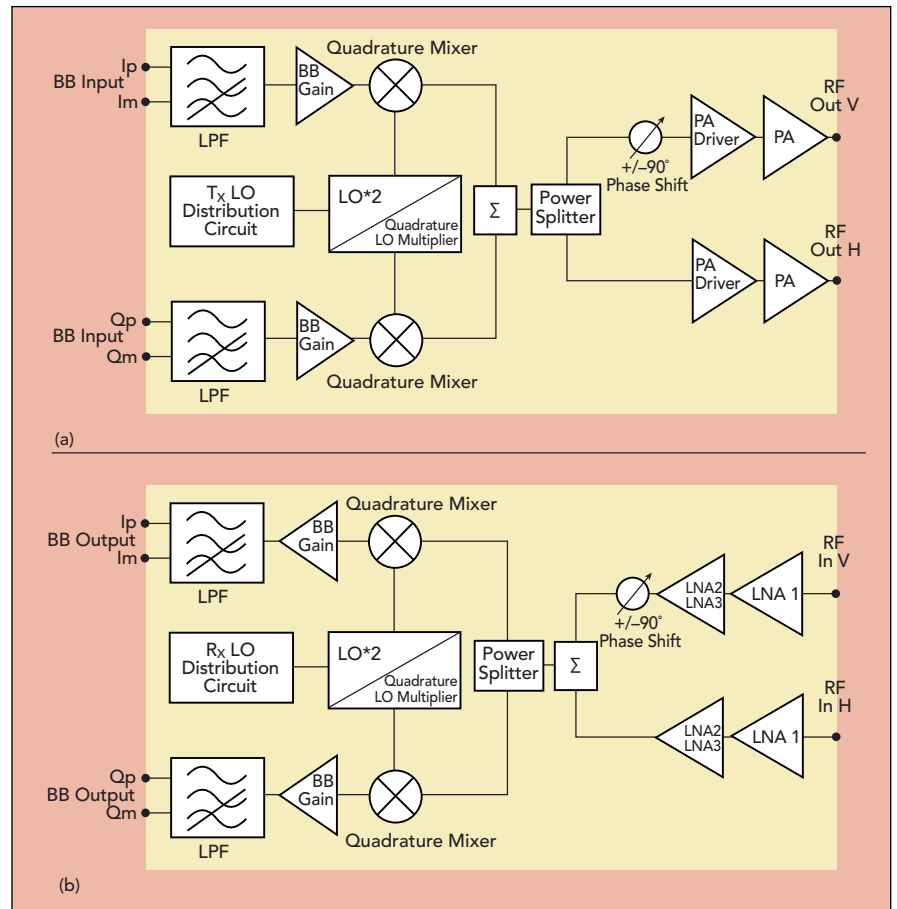
A companion to the Prime DBF, Satixfy's first-generation RFFE is a Ku-Band RFIC which links the Prime's I/Q signals with the Ku-Band antenna elements (see **Figure 7**). Called Beat, the RFFE integrates the transmit driver and power amplifier, transmit up-converter, receive low



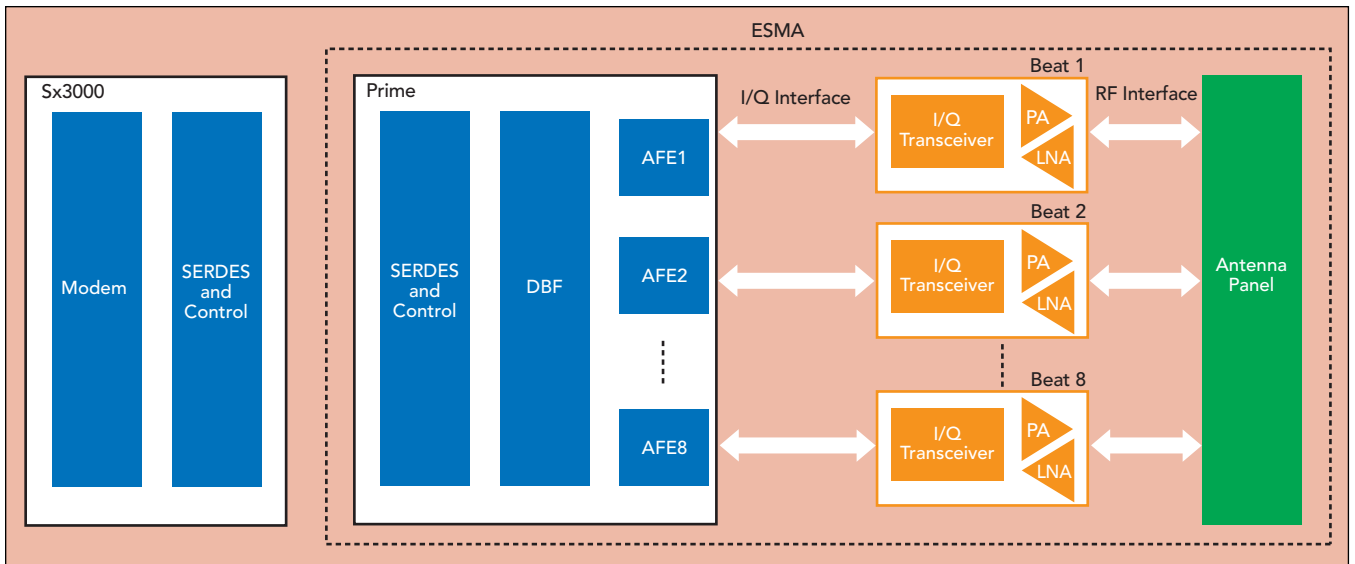
▲ Fig. 6 Prime DBF capability: number of beams vs. bandwidth.



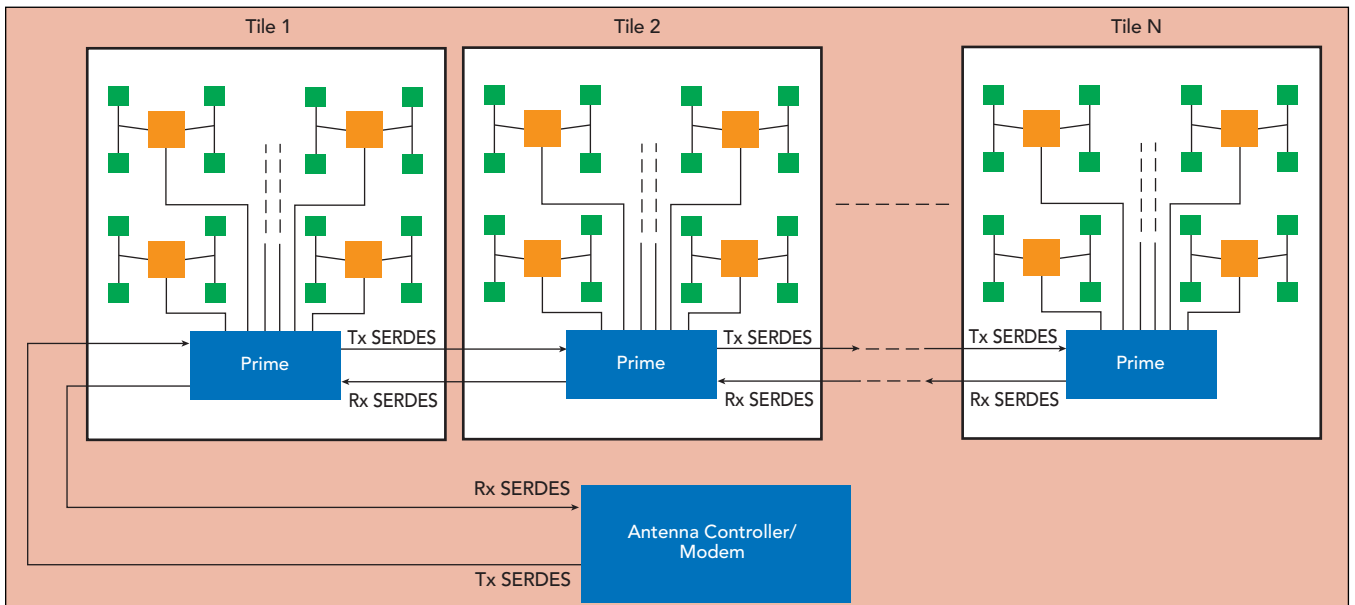
▲ Fig. 7 SatixFy Beat Ku-Band front-end.



▲ Fig. 8 Block diagram of a single element, circularly polarized Tx (a) and Rx (b).



▲ Fig. 9 System architecture.



▲ Fig. 10 Tiled ESMA to increase aperture size.

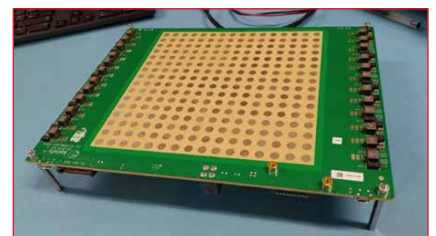
noise amplifier, receive down-converter and antenna polarization control, either linear or circular (see **Figure 8**). A single Beat supports four Ku-Band antenna elements operating in half-duplex mode.

Figure 9 shows the block diagram of a fully integrated ESMA system composed of the Prime DBF, Beat RFFE and the antenna panel. The Prime DBF at the heart of the electronically-steerable antenna is connected to the Beat RFFE via an analog I/Q interface and to the Sx3000 modem via high speed SERDES. This level of integration enables a highly configurable antenna supporting different applications. Within this architecture, the DBF is band-agnostic, meaning to build phased array antennas for different satellite (Ku-, Ka- or X-Band) or 5G (sub-6 or 28 GHz) bands, only the RFFE and antenna panel need to be modified. The backbone of the BFN remains the same, greatly simplifying antenna designs for different applications and frequency bands. For phased array antennas at VHF and UHF, Prime can be used with an

LNA and PA without up- or down-converters.

The modular architecture of the ESMA enables it to be scaled to larger arrays by tiling. An example is shown in **Figure 10**, where a single tile of 32 antenna elements requires eight Beats and one Prime. The tiles are daisy-chained via high speed SERDES, which provides both data and the control plane to and from the antenna controller.

SatixFy recently introduced the world's first fully digital 256-element ESMA for Ku-Band SATCOM (see **Figure 11** and **Table 1**). The ESMA antenna can serve both as a standalone IoT terminal or a building block for a larger array. The antenna is a single board design



▲ Fig. 11 Ku-Band 256-element ESMA.

TABLE 1
Ku-BAND ESMA

Topology	Tx/Rx Half Duplex TDD
# Beams	Up to 32 Simultaneous Beams
Frequency Coverage	Rx: 11 to 12 GHz Tx: 13.75 to 14.5 GHz
# Elements	256
# DBFs	8 Primes
# RFICs	64 Beats
RF Bandwidth	1 GHz
Channel Bandwidth	880 MHz
Tx Antenna Gain	28 dBi
Rx Antenna Gain	26.5 dBi
Modem	Sx 3000-Based Modem
Digital Interconnectivity	4 SerDes Lanes at 9.4 Gbps/Lane
Terminal Functionality	Self-Sufficient System, Single Board Design, Minimal External Interfaces

with a shared aperture antenna (Rx and Tx), operating from 11 to 12 GHz for Rx and 13.75 to 14.5 GHz for Tx. The 256-element ESMA comprises eight Primes daisy-chained and 64 Ku-Band Beats. The antenna can simultaneously point, track and manage multiple beams with multiple polarizations. **Figure 12** shows the antenna radiation patterns, measured in an anechoic chamber.

APPLICATIONS

The flexible ESMA architecture enables low-cost, adaptive and steerable antenna system with low weight and power consumption. This makes this system viable and attractive for various applications:

IoT

In rural areas, satellites can provide the missing coverage to connect sensors and other entities to the cloud, such as sensors for agriculture, water metering, weather, petrol and gas metering. The ESMA enables

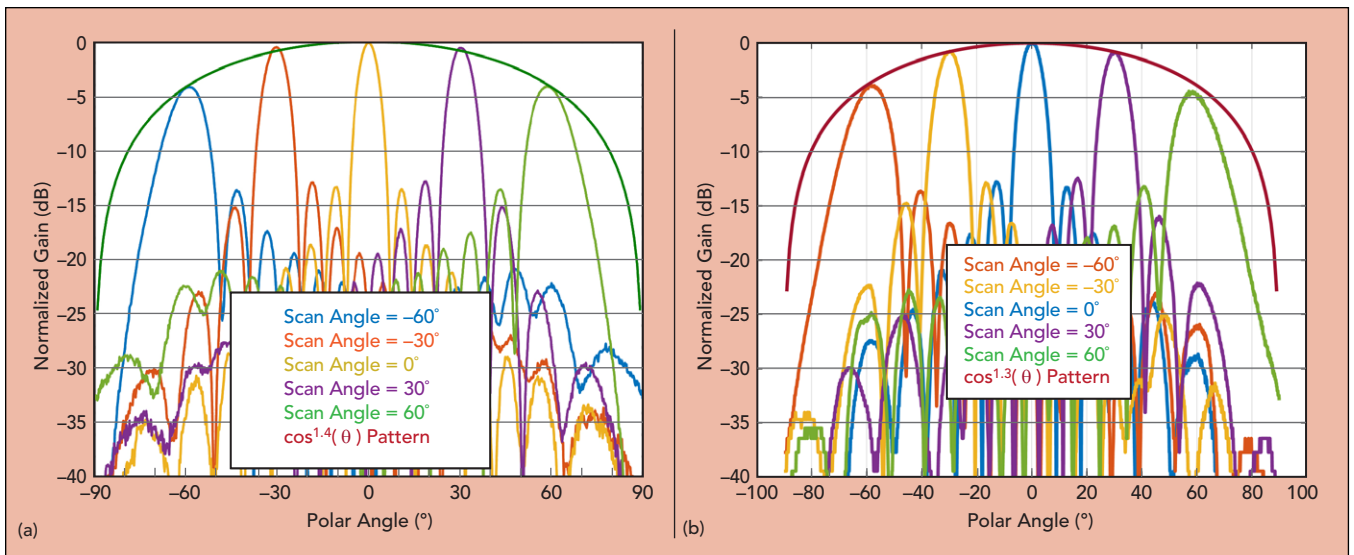
compact, low-cost and low-power IoT antennas that can automatically search, acquire and track satellites. Advantages of the ESMA include eliminating bulky mechanical structures and self-installation and tracking, which significantly reduce installation cost and enables mobile applications on vehicles, ships, aircraft and drones. The small antenna size is feasible using appropriate waveforms,¹⁻² making it possible to communicate at very low SNR.

Broadband Communications for Land, Maritime and Aeronautical Applications

High capacity GEO networks and new constellations of LEO and MEO satellites will help serve the demand for broadband access, both for fixed terminals in remote areas and SOTM applications. During the past decade, the demand for broadband connectivity and inflight entertainment on commercial airlines has demonstrated the need for low drag and highly reliable antenna systems, making a conformal antenna based on ESMA a good solution. The simultaneous multi-beam capability enables simultaneous connectivity with multiple satellites and make-before-break connections to ensure seamless connectivity—particularly when switching beams with LEO satellites at high speed. These same benefits extend to land mobile and maritime applications, where ESMA based SATCOM links can co-exist with terrestrial wide area communications. The ESMA can be scaled according to the required link budget, physical size, weight and power consumption constraints of the platform.

5G Fixed Wireless Access

The jump in 5G data rates, compared to 4G, relies on smart antennas with multiple, wideband, directive beams. ESMA’s beamforming capability can increase spectrum utilization by up to two orders of magnitude. The high precision phase shifters and TTD in the DBF makes it suitable for the both mmWave and sub-6 GHz arrays. The ESMA’s flexibility enables dynamically reconfiguring the beams, combined with 1D and 2D dual-polarized scanning for both line-of-sight



▲ Fig. 12 Measured 256-element ESMA H-plane radiation patterns vs. scan angle: Tx at 13.75 GHz (a) and Rx at 11.7 GHz (b).

and non-line-of-sight channel conditions. With TTD beamforming, high gain and squint free antenna patterns can be achieved across the entire cellular band.

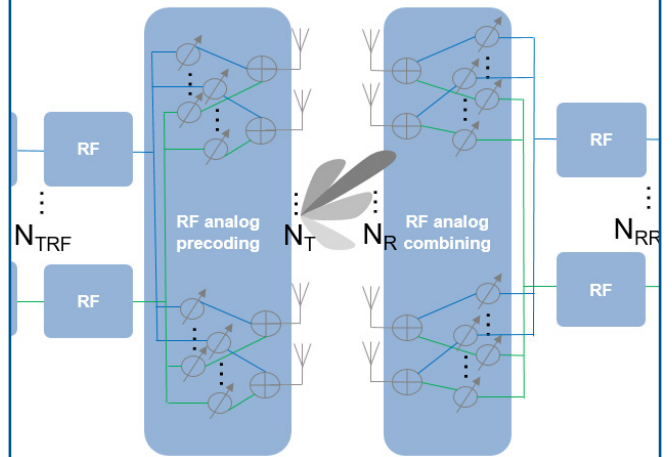
SUMMARY

This article introduced a scalable ESMA with two building blocks: a digital ASIC (Prime) with TTD, which performs the signal processing and beamforming, and an RFFE containing the RF amplification and up- and down-conversion, which is the interface between the DBF and the antenna element. The chipset enables a flexible and scalable architecture, with the resulting ESMA achieving extremely small size, low power consumption and low-cost, compared to other approaches. Products based on ESMA will support a wide range of applications, including SATCOM (GEO, LEO and MEO) and 5G.

References

1. D. Rainish and A. Freedman, "VLSNR Implementation for Mobile Broadband Application," *21st Ka and Broadband Communications Conference*, Bologna, Italy, October 2015.
2. A. Freedman and D. Rainish, "Air Interface for Low Power Operation of a Satellite Terminal," *21st Ka and Broadband Communications Conference*, Bologna, Italy, October 2015.

Introduction to Hybrid Beamforming and System Simulation



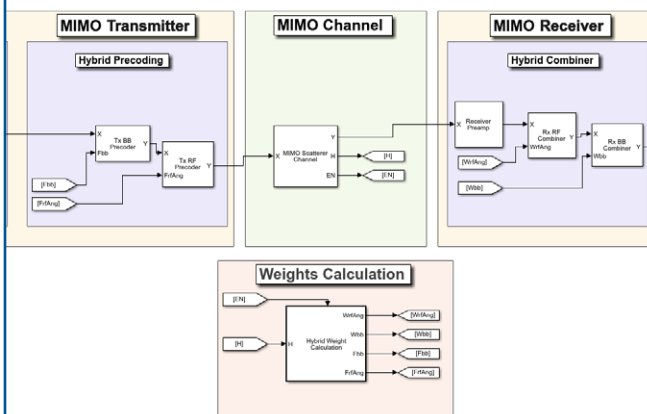
Get MATLAB® and get started.

mathworks.com/example-beamforming



Hybrid MIMO Beamforming with QSHB and HBPS Algorithms

Hybrid MIMO Beamforming with Sparse Beamspace Precoding

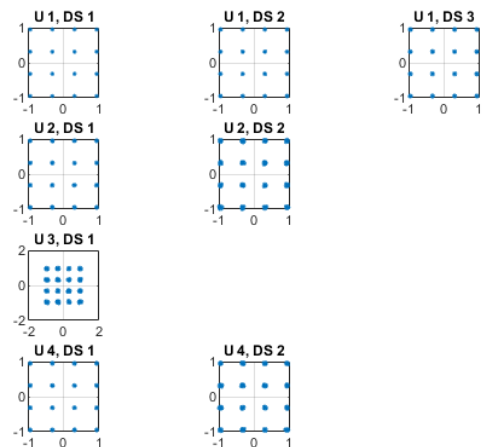


Get MATLAB® and get started.

mathworks.com/example-qshb



Massive MIMO Hybrid Beamforming Transmission Design



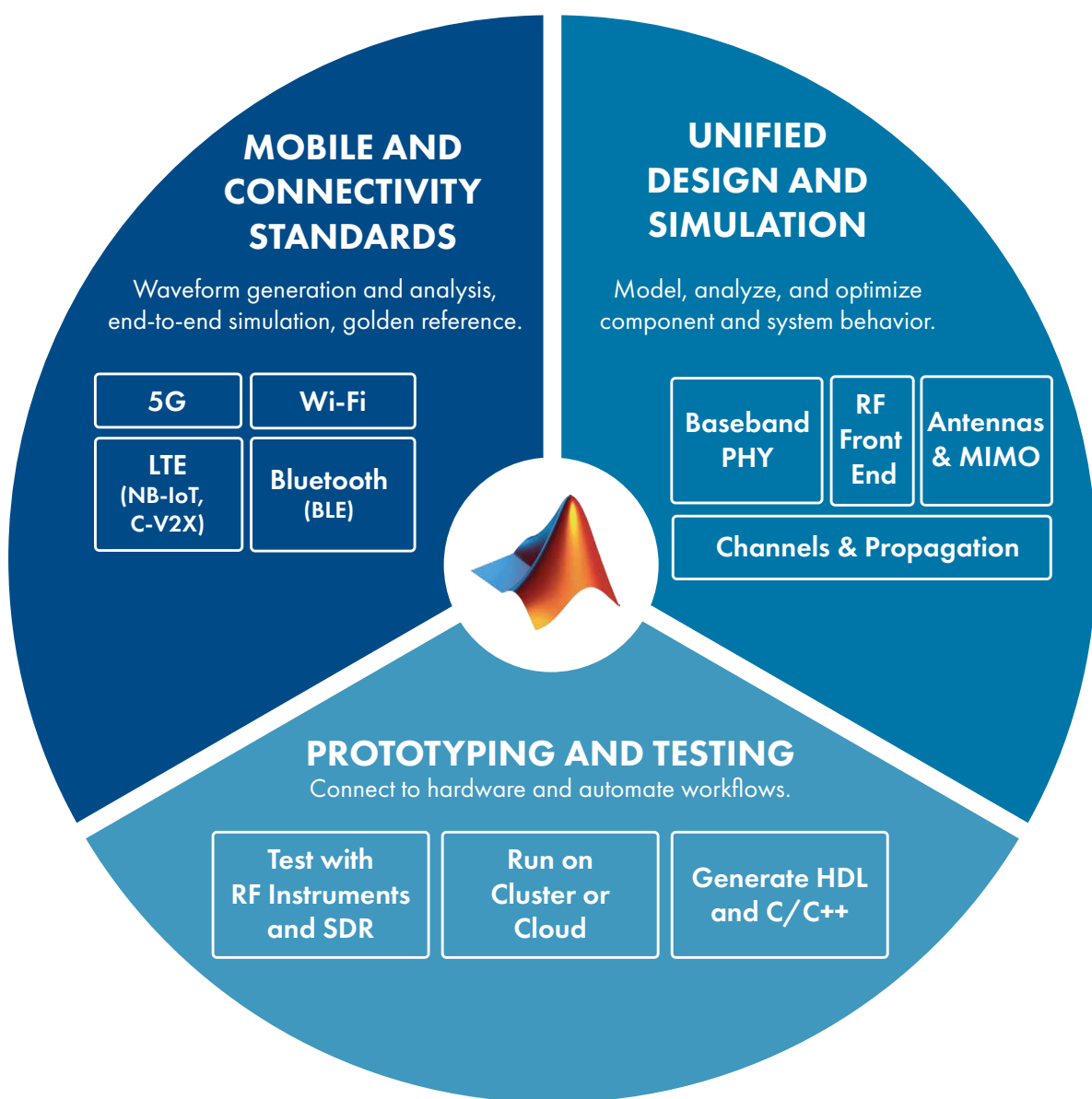
Get MATLAB® and get started.

mathworks.com/example-mimo-beam



MATLAB and Simulink for WIRELESS DESIGN

Explore how you can reduce development time, eliminate design problems early, and streamline testing and verification.



mathworks.com/wireless-design